APPLICATIONS OF LANDSAT-5 TM IMAGERY IN ASSESSING AND MAPPING WATER QUALITY IN BANKHEAD RESERVOIR OF THE BLACK WARRIOR RIVER

by

DOROTHY COLLEEN FORRER

LUOHENG HAN, COMMITTEE CHAIR
ROBERT FINDLAY
MICHAEL STEINBERG

A THESIS

Submitted in partial fulfillment of the requirements
for the degree of Master of Science
in the Department of Geography
in the Graduate School of
The University of Alabama

TUSCALOOSA, ALABAMA

2012

ABSTRACT

Bankhead Reservoir of the Black Warrior River is designated for swimming (S), fish and wildlife (F&W), and to be used as a public water source (PWS). The water quality of Bankhead is impacted by both point and nonpoint source pollution. Only a limited number of intensive studies have been conducted on Bankhead Reservoir due to the cost and resources necessary to sample areas distributed throughout the entire system. This research uses remote sensing technologies coupled with a limited number of *in situ* water samples to estimate and map the concentrations of total suspended solids and chlorophyll-*a* in Bankhead Reservoir using Landsat TM data. The principle behind the technique used implements spectral reflectance to predict water quality variables via different regression models. The results from this study serve as baseline water quality maps that can be used for comparison in future monitoring. A land use/land cover map was created of the study area to briefly investigate potential land use related causes of water quality variation. The use of remote sensing allows for a more synoptic view of total suspended solids and chlorophyll-*a* concentrations in Bankhead Reservoir for both spring and summer conditions.

ACKNOWLEDGMENTS

I would like to thank David Deyton, Jacob Richards, and my family for the never-ending support and encouragement needed to succeed. I would also like to thank Nelson Brooke and Charles Scribner, with Black Warrior Riverkeeper, for providing the boat and means to gather water samples used in analysis. I am most indebted to Dr. Luoheng Han, the thesis committee chairman, for sharing his expertise and wisdom regarding water quality mapping using remote sensing technologies as well as for his support of my thesis and academic progression. I would also like to thank Dr. Robert Findlay and Dr. Michael Steinberg for serving on my thesis committee and providing invaluable research guidance.

CONTENTS

LIST OF TABLES

LIST OF FIGURES

1. Introduction

The quality of freshwater resources in the United States is of increasing concern as population and industrial activity continue to grow. Though surface water quality is influenced by natural factors such as geology, climate, vegetation, and morphology, anthropogenic activities contribute significantly to water pollution. Water quality is impacted through both point and nonpoint source pollution. The Clean Water Act (1972) set forth the initial framework for regulating the discharge of pollutants into surface waters and enabled the Environmental Protection Agency (EPA) to establish water quality standards to be upheld through regular monitoring carried out by individual state agencies. The Alabama Department of Environmental Management (ADEM) is the chief agency in charge of enforcing the water protection measures mandated by the CWA for the State of Alabama. ADEM administers the National Pollutant Discharge Elimination System (NPDES) to regulate point sources of water pollution from facilities. Several facilities have NPDES permits issued by ADEM to discharge wastewater into Bankhead Reservoir including industrial and commercial facilities (ADEM 2004c). Activities that disturb the earth's surface such as logging, construction, road building, and mining create a further threat within the watershed from nonpoint source pollution (ADEM 2004c). Nonpoint sources are much more difficult to monitor and the Nonpoint Source Program in Alabama has no federal regulation and relies on a voluntary approach to control. With more than 120,000 kilometers of rivers and streams and over 190,000 hectares of public lakes and reservoirs, Alabama is recognized for its wealth of freshwater resources. Effectively monitoring and assessing the conditions of the state's abundant surface waters is an incredible challenge.

In 2010, the United States produced 1,084.4 million tons of coal; Alabama is a significant contributor with eight underground coalmines and forty-two surface coalmines (EIA 2010). Approximately ninety-five percent of the coalmines found in Alabama are located within the

Black Warrior Watershed (ADEM 2004a). A report issued by the conservation group *American Rivers* placed the Black Warrior River on the 2011 annual list of *America's Most Endangered Rivers* due to coal mine related pollution (American Rivers 2011). Bankhead Reservoir is the northernmost impoundment on the Black Warrior's main stem and is located near the center of the Warrior Coal Field, the largest coalfield in Alabama. ADEM designates Bankhead Reservoir to be used for swimming, fish and wildlife, and as a public water source (ADEM 2010). Shoal Creek Mine, one of the largest underground coal mines in Alabama, is located along and underneath portions of Bankhead Reservoir and has an NPDES permit to legally discharge wastewater directly into the lake and its major tributaries (ADEM 2009). It is imperative that Bankhead Reservoir is effectively monitored to ensure it is meeting its designated uses and to identify and understand potential water quality threats that could be of future concern. Under ADEM's current monitoring program, intensive water quality surveys are the most thorough assessments conducted on public reservoirs but are sampled on a rotating basin approach only once every five years (ADEM 2005). Only a limited number of intensive studies have been conducted on Bankhead Reservoir due to the cost and resources necessary to sample areas distributed throughout the entire system.

Over the last several decades remote sensing technologies have been improved and successfully implemented to assess water quality conditions. Unlike *in situ* measurements alone, remote sensing allows for a synoptic view that improves estimations of large areas and is capable of identifying pollution problems critical for effective surface water management (Ritchie *et al*. 2003). Water bodies can be monitored completely, on a regular basis, and in a cost-effective way using remote sensing technologies. Applications of the Landsat Thematic Mapper (TM) sensor have been widely implemented to establish relationships between surface reflectance and water quality parameters of inland water bodies. It has successfully been used to estimate and map the spatial distribution of water quality parameters such as chlorophyll-*a* and total suspended solids (TSS) in surface waters (Ritchie *et al.* 1990, Dekker and Peters 1993, Han and Jordan 2005, Wang *et al.* 2006). Regression is most frequently chosen to demonstrate the relationship between the spectral reflectance of surface water measured by sensors and near simultaneous *in situ* water quality measurements.

The purpose of this research is to estimate and map the concentration of TSS and chlorophyll-*a* in Bankhead Reservoir using Landsat TM data. The principle behind the technique used is to implement spectral reflectance to predict the water quality variables, i.e., TSS and chlorophyll-*a* via different regression models. The results from this study serve as baseline water quality maps providing a complete spatial view of TSS and chlorophyll-*a* concentrations that can be used for comparison in future monitoring. The maps allow for a preliminary assessment of the potential impact Shoal Creek Mine pose on Bankhead Reservoir and a land use/land cover map was created of the study area to briefly investigate other potential land use related causes of water quality variation. The use of remote sensing techniques allows for a more synoptic spatial view of total suspended solids and chlorophyll-*a* concentrations in Bankhead Reservoir for both spring and summer conditions.

2. Literature Review

2.1 Water Quality Standards

The Clean Water Act is the foundation for national surface water protection and aims to restore and maintain the nation's waters to support "the protection and propagation of fish, shellfish, and wildlife and recreation in and on the water" (1972). Water quality standards resulted as a way of enacting the extensive goals of the CWA into acceptable objectives for individual water bodies and are used as a reference for monitoring. Under the CWA, a federal-state partnership exists in which the federal government's jurisdiction is broad (EPA 2008). The EPA delegates the monitoring and enforcement of surface water protection to state environmental agencies; ADEM is the chief environmental agency for Alabama.

The term water quality refers to the chemical, physical, and biological characteristics of water (Liu et al. 2003). Qualified states are responsible for establishing state water quality standards as well as issuing industrial and municipal discharge permits. Water quality standards consist of setting the designated uses of a water body (fish and wildlife, public water source, etc), establishing water quality criteria for maintaining those uses, and following an anti-degradation policy for its protection (ADEM 2011a). Designated use classifications "apply water quality criteria adopted for particular uses based on existing utilization, uses reasonably expected in the future, and those uses not now possible because of correctable pollution but which could be made if the effects of pollution were controlled or eliminated" (ADEM 2011b). ADEM sets water quality criteria that must be met by all state waters but also specifies particular criteria based on a water bodies use classification. Water bodies with different designated uses potentially may be required to meet different water quality criteria. For example, according to ADEM, Agricultural and Industrial Water Supply (A&I) designations are required to maintain a lower level of dissolved oxygen compared to Fish and Wildlife (F&W) designations. The anti-degradation policy set forth by ADEM "serves to conserve and protect the waters of Alabama and their beneficial uses to prevent the deterioration of a water body even when its water quality surpasses necessary level to meet the fishable/swimmable goals of the Clean Water Act" (ADEM 2011a).

Under Section 314 of the CWA (1972), states are required to monitor all publicly owned lakes to determine if water quality standards are being met and to identify those water bodies not supporting their designated standards. Each state must submit those findings in a biennial Integrated Water Quality Report to Congress in order to ensure that surface water quality standards are upheld as well as to mitigate problems causing impairment (EPA 2008). ADEM implements lake assessment through the Rivers and Reservoirs Monitoring Program to ensure Alabama public reservoirs are sampled at least once every two years to meet the requirements of Section 314 of the CWA (ADEM 2005). Waters not supporting their designated use(s) are regarded as impaired and placed on Alabama's 303(d) list. The 303(d) list reports each segment of impaired water bodies, the reason and origin of impairment, and proposes a deadline for developing a Total Maximum Daily Load (TMDL) or maximum pollutant limit a water body can receive and still uphold water quality standards (EPA 2008).

2.2 ADEM Rivers and Reservoirs Monitoring Program

The Rivers and Reservoirs Monitoring Program evaluates the water quality of Alabama publicly-owned lakes/reservoirs and non-wadeable rivers. ADEM designed the program for monitoring on three different levels: intensive monitoring, compliance monitoring, and critical period monitoring (ADEM 2005). Alabama's forty public lakes are divided into five basins and intensive monitoring of each basin is conducted April-October on a five-year rotating schedule;

thus, lakes and reservoirs are intensively monitored only once every five years (ADEM 2005). The intensive water quality survey samples both main-stem reservoir and tributary embayment stations providing the most comprehensive assessment of water quality. Bankhead Reservoir is in the Warrior Basin and was most recently intensively surveyed in 2007, but the results from that study are still not available from ADEM. Compliance monitoring samples main-stem locations of reservoirs with established nutrient criteria April-October once every three years (ADEM 2005). Bankhead Reservoir has established nutrient criteria in the dam forebay and, along with the reservoir's other main-stem stations, is sampled every three years under compliance monitoring. If a reservoir is not scheduled for intensive or compliance monitoring, reservoir main-stem locations are sampled in August only. Critical period monitoring ensures every public reservoir is monitored at least once every two years to meet the requirements of the CWA (ADEM 2005).

The objectives of this program are to create and uphold a database of water quality for all rivers and public lakes in order to provide a comprehensive assessment, study trends in lake trophic status through long-term monitoring, and meet requirements of Section 314 of the CWA to conduct biennial water quality assessments for all public lakes and reservoirs (ADEM 2005). The program does succeed in meeting the qualifications of the CWA, but it is unable to provide a truly comprehensive temporal and spatial view of water quality within entire reservoirs. While the intensive monitoring survey does provide the most complete approach to assessing the water quality of entire Alabama reservoir systems, this intensive assessment occurs only once every five years. With the growing number of point source discharges and nonpoint source pollution entering surface waters, a synoptic view of river and lake water quality is extremely useful in effective management and needed more often than every five years to understand and detect probable water quality concerns.

2.3 Water Quality Parameters: Total Suspended Solids and Chlorophyll-a

The EPA defines suspended and bedded sediments (SABS) as "organic and inorganic particles that are suspended in, are carried by the water, or accumulate in water bodies. This definition includes the frequently used terms clean sediment, suspended sediment, total suspended solids, turbidity, bedload fines, deposits or, in common terms, soils or eroded material" (EPA 2006). Total suspended solids are particles found in the water column that cannot pass through a 2-micron filter and are comprised of silt and clay particles, plankton, algae, fine organic debris, and other particulate matter (Berry *et al*. 2003). According to the EPA, suspended solids are a unique water quality problem compared to other water pollutants because they are important for the ecological function of the water body and are found naturally in background amounts (EPA 2006). In natural amounts suspended sediments are vital for sediment bedload replenishment and help to create aquatic micro-habitats. For suspended solids management it is important to understand and maintain background levels within a water body to effectively protect aquatic life (EPA 2006).

Typically, TSS concentration is correlated with discharge and the 2002 Intensive Water Quality Study of Black Warrior River Reservoirs found that TSS in most cases was controlled by the rate of discharge at the time of sampling. Elevated concentrations of suspended matter can indicate river erosion and can affect light penetration, quality of aquatic habitat, and recreational values of the lake. Increased amounts of suspended solids in surface water bodies can act as transports of toxic pollutants and could also indicate further water quality impairment (Berry *et al.* 2003). Sedimentation can cause river and stream channels to fill in and flood more easily and can make river water harder to purify for use as drinking water. Sources of suspended solids come from both point and nonpoint sources including: industrial discharges, sewage, fertilizers, road runoff, and soil erosion (Berry *et al*. 2003). ADEM does not require numeric TSS criteria to support designated uses of surface water but addresses suspended material through turbidity criteria. Turbidity measures the decreased passage of light due to the amount of suspended particles in the water. According to ADEM's water quality criteria for specific designated uses of water bodies, in Bankhead Reservoir "there shall be no turbidity of other than natural origin that will cause substantial visible contrast with the natural appearance of waters or interfere with any beneficial uses they serve. In no case shall turbidity exceed 50 Nephelometric units above background" (ADEM 2011a). TSS is not sampled during winter months when it is most likely to be elevated and a potential threat.

Chlorophyll-*a* is a pigment found in all plants and algae and is commonly used as an indicator of water quality. Eutrophication refers to the natural and anthropogenic increase of plant nutrients into a water body and the impacts elevated nutrients have on aquatic ecosystems (National Academy of Sciences 1969). Due to elevated nutrients, algae increases productivity and biomass, potentially limiting light penetration and dissolved oxygen levels. Chlorophyll-*a* provides an estimate of algal biomass concentrations and indicates the biological production found within a water body (Hambrook *et al*. 2007). Algal organic matter is approximately 1.5% chlorophyll-*a* and phytoplankton biomass can be estimated if chlorophyll-*a* levels in the water body are known (APHA 1989, Raschke 1993).

Cultural eutrophication is the primary water quality concern and occurs due to over-enrichment resulting from anthropogenic activities (ADEM 2009b). Cultural eutrophication has continued to increase with the growth of population, industrialization, and rigorous agricultural and forestry practices (AFA 1996). Lakes have variable responses to nutrient inputs and therefore ADEM implements water body-specific criteria to enhance nutrient management (ADEM 2011a). ADEM utilizes chlorophyll-*a* as the primary indicator of cultural eutrophication and as a means of protecting the designated uses of lakes and reservoirs from nutrient impairment (ADEM 2009b). For Bankhead Reservoir the "mean of the photic-zone composite chlorophyll a samples collected monthly April through October shall not exceed 16 μgl^{-1}, as measured at the deepest point, main river channel, dam forebay" (ADEM 2011a). Fish growth and biomass most likely benefit as chlorophyll-*a* increases to moderately eutrophic levels (10-15 μgl^{-1}); however, exceeding these limits may cause water quality as well as fish habitats to decline (Bayne *et al*. 1994). According to Raschke, (1993) chlorophyll-*a* levels ranging from 10-15 μgl^{-1} discolor the water and algal scums may develop, levels ranging from 20-30 μgl^{-1} deeply discolor the water, algal scums are frequent, and algal matting may occur.

2.4 Point and Nonpoint Source Pollution

Water pollution impairs surface waters potentially making it hazardous for drinking, fishing, swimming, and other recreational activities. The two sources of water pollution are from point and nonpoint sources. Defined in the CWA (1972), "a point source means any discernible, confined and discrete conveyance, including but not limited to any pipe, ditch, channel, tunnel, conduit, well, discrete fissure, container, rolling stock, concentrated animal feeding operation, or vessel or other floating craft, from which pollutants are or may be discharged". In Alabama, point source pollution is monitored through the National Pollutant Discharge Elimination System (NPDES) regulating program and overseen by ADEM. The NPDES identifies and regulates direct sources of pollutants into surface waters, including both industrial and municipal dischargers. Shoal Creek Mine has sixty-one permitted industrial discharges with ten discharging directly into Bankhead Reservoir (ADEM 2009a). Municipal Separate Storm Sewer Systems (MS4s) must obtain a municipal NPDES permit and transport untreated polluted stormwater runoff, in towns and cities across Alabama, and subsequently released into receiving water bodies.

Nonpoint source pollution is created when precipitation moves across the earth's surface and runoff picks up pollutants that are eventually deposited in surface waters. According to the EPA, nonpoint source pollution is a leading cause of water quality impairment and includes "excess fertilizers, herbicides, and insecticides from agricultural lands and residential areas; oil, grease, and toxic chemicals from urban runoff and energy production; sediment from improperly managed construction sites, crop and forest lands, and eroding stream banks; salt from irrigation practices and acid drainage from abandoned mines; bacteria and nutrients from livestock, pet wastes, and faulty septic systems" (EPA 1994). Urban areas contain impervious surfaces, which can altar hydrology and geomorphology of streams and increase runoff. Urban runoff carries higher nutrient loads (Emmerth and Bayne 1996, Rose 2002), sediment loadings (Wahl *et al*., 1997), and other pollutants into nearby stream waters. States are provided funds from a federal program to develop programs that strive to reduce nonpoint source pollution. However, unlike point source regulation the Nonpoint Source Program in Alabama has no federal regulation and relies on a voluntary approach to control. Bankhead Reservoir is impacted by nonpoint source pollution but it is diffuse and much more difficult to monitor and regulate.

2.5 Shoal Creek Mine

Shoal Creek Mine is an underground bituminous coal mine located along and underneath segments of Bankhead Reservoir near the center of the Warrior Coal Basin. Underground coal is mined here using longwall and continuous mining methods. Longwall mining can extract in excess of 1,000 ft. (305 m) wide and over 8,000 ft. (2438 m) long rectangular blocks of coal (EIA 2005). For every 1,000 tons of coal produced by longwall underground mining a little over one and a half tons of liquid waste effluent is created (World Bank Group 1998). There is a two thousand ton-per-hour jig preparation plant capable of washing eleven million tons of raw coal yearly located on site at Shoal Creek Mine according to the owner, Drummond Company.

Coal washing creates a significant amount of wastewater and Shoal Creek Mine has sixty-one permitted wastewater discharges; ten of those inputting directly into Bankhead Reservoir (ADEM 2009a). Coal mining wastewater effluent is not free from pollutants and is high in TSS, oil and grease and can impact the chemical quality of receiving surface waters (Tiwary and Dhar 1994). NPDES permits provide guidelines for voluntary Best Management Practices to clean wastewater but allow designated levels of pollutants. Shoal Creek Mine's NPDES permit (AL0062421) has designated TSS, lead, manganese, and pH effluent limits to ensure discharges do not exceed maximum allowable levels. However, according to their permit issued by ADEM, increased storm water discharges after twenty-four precipitation events are exempt from meeting effluent limitations for at least twenty-fours after the event (ADEM 2009a). Exempting permit regulations and ignoring limits is essentially allowing the mine to pollute legally. If total suspended solids are elevated too high it can degrade streams and reduce biodiversity if not mitigated.

The mine and the preparation plant use truck haul roads, rail lines, and river transport systems to move various materials created in processing coal from underground mining. Roads and rail are used to carry coal and overburden outside of the mining area. Vegetation removal and soil grading was required for construction which potentially increases offsite sediment discharge in stormwater runoff (EPA 1995). Pollutants found in stormwater discharge include acids, suspended solids, dissolved solids, iron, manganese, and traces of other metals (EPA 1995). Shoal Creek Mine is an extensive operation and its numerous permitted discharges are also intended to control excess runoff of pollutants from the mining area. However, ADEM exempts this mine from regulating pollutants in storm water discharge following twenty-four rain events; a period when regulations are needed the most to protect Bankhead Reservoir and surrounding tributaries (ADEM 2009a).

2.6 Remote sensing of water quality using the Landsat TM sensor

Remote sensing techniques do not eliminate *in situ* sampling entirely but can be used to quantify water quality parameters for an entire water body from a relatively small number of samples. The Landsat TM sensor's temporal coverage, spatial resolution, and data accessibility make it especially useful for monitoring inland water bodies (Kloiber *et al.* 2002; Zhou *et al.* 2006). The revisit cycle of the sensor is sixteen days for a particular area. The sensor records electromagnetic radiation in seven individual bands able to produce digital images of earth's surface. Each Landsat scene has 30-meter ground resolution for bands 1,2,3,4,5,7 and 120 meter for band 6 and covers approximately 185 by 170 kilometers of the earth's surface. Table 1 was adapted from Jenson (2000) and lists the Landsat-5 TM radiometric characteristics. The USGS Global Visualization Viewer (GloVis) is an online search and order tool for satellite data that enables users to easily access and download currently available Landsat 1-5 MSS, Landsat 5 TM, Landsat 7 ETM+, Aster, and MODIS data for free.

Table 1 Characteristics of Landsat-5 TM bands (Adapted from Jenson 2000)
NIR, near infrared; SWIR, short wavelength infrared

Band	Spectral region	Wavelength (µm)	Centre Wavelength (µm)	Spatial Resolution (m)
1	Blue	0.42-0.52	0.485	30 x 30
2	Green	0.52-0.60	0.56	30 x 30
3	Red	0.63-0.69	0.66	30 x 30
4	NIR	0.76-0.90	0.86	30 x 30
5	SWIR	1.55-1.75	1.65	30 x 30
7	SWIR	2.08-2.35	2.22	30 x 30

The Landsat TM sensor is currently used to measure TSS and chlorophyll-*a* found in surface water. The majority of researchers have concluded that the concentration of total suspended solids (Schiebe *et al.* 1992; Dekker and Peters 2002; Wang *et al*. 2006; Zhou *et al.* 2006) and chlorophyll-*a* (Ritchie *et al.* 1990; Ekstrand 1998; Schiebe *et al.* 1992; Giardino *et al*. 2001, Han and Jordan 2005) can be mapped for large water bodies using currently available sensor data. Landsat TM bands 1-4 are within the spectral range (400-900 nm) able to penetrate water and thus capable of providing useful water quality information (Dekker and Peters 1993).

Suspended sediments in surface water increase the spectral radiance of the visible light and near-infrared portions of the electromagnetic spectrum (Ritchie *et al*. 1976). Results of a study estimating total suspended solids from remotely sensed water reflectance conducted by Novo *et al*. (1991) proved that there is a significant and constant correlation between spectral reflectance from 450-900 μm and TSS; however, the "rate of change in spectral reflectance with TSS peaked in the red region". Chlorophyll-*a* has distinct absorption and scattering characteristics with strong absorption between 400 and 500 nm and also 680 nm with peak reflectance at 550 nm and 700 nm (Han 1997). Many studies have successfully estimated water quality concentrations by implementing regression models with single TM bands and band ratios as independent variables (Ritchie *et al.* 1990, Lathrop 1992, Dekker and Peters 1993, Wang *et al.* 2006). Different band and band ratios have been found to successfully estimate a single water quality parameter (Wang *et al*. 2006). Choosing which bands, band ratios and/or combination of bands to use in regression can be a challenging process (Han and Jordan 2005).

Several studies have been conducted implementing remote sensing technologies to estimate total suspended solids in surface waters. Lathrop conducted an investigation on the relationship between water quality and spectral reflectance and concluded band ratios TM2/TM1 and TM3/TM1 had the strongest relationship to total suspended solids (1992). In a study mapping total suspended matter (TSM) in Lake Taihu, China, Zhou *et al*. found TM3 was the most significant predictor of TSM during different seasons regardless of algae concentration (2006). Total suspended matter is another term for total suspended solids. The average of bands TM2 and TM3 has also been used to establish the relationship between total suspended solids and spectral radiance (Dekker *et al.* 2002).

According to Dekker and Peters (1993), Band 4 reflectance is "the product of rapidly increasing water absorption and probably suspended matter reflection". Ekstrand concluded that TM band 4 could be implemented to successfully estimate surface water chlorophyll-*a* concentrations in coastal waters (1998). Band ratios have been proven especially useful for establishing the relationship between chlorophyll-*a* concentrations due to its characteristic scattering and absorption properties (Dekker *et al.* 1991). Han and Jordan implemented the band ratio TM1/TM3 to estimate and map chlorophyll-a concentrations in Pensacola Bay, Florida (2005). In a similar study, Wang *et al.* found the band ratio TM3/TM2 best explained the variance of chlorophyll-*a* concentration in Reelfoot Lake, Tennessee (2006). Band ratio TM1/TM2 has also been successfully implemented to establish an empirical relationship used to map chlorophyll-*a* concentration (Dwivedi and Narain 1987).

Traditional water point sampling alone can be expensive to efficiently monitor heterogeneous water bodies. Remote sensing allows a fewer number of samples necessary to provide an overview of water quality conditions for the entire water body and not only the *in situ* sample points. The goal of remote sensing of surface water bodies is to gain a truly synoptic view of water quality conditions. Remote sensing techniques also provide water quality information for areas that are otherwise difficult or impossible to access in the field.

3. Methodologies

3.1 Study area

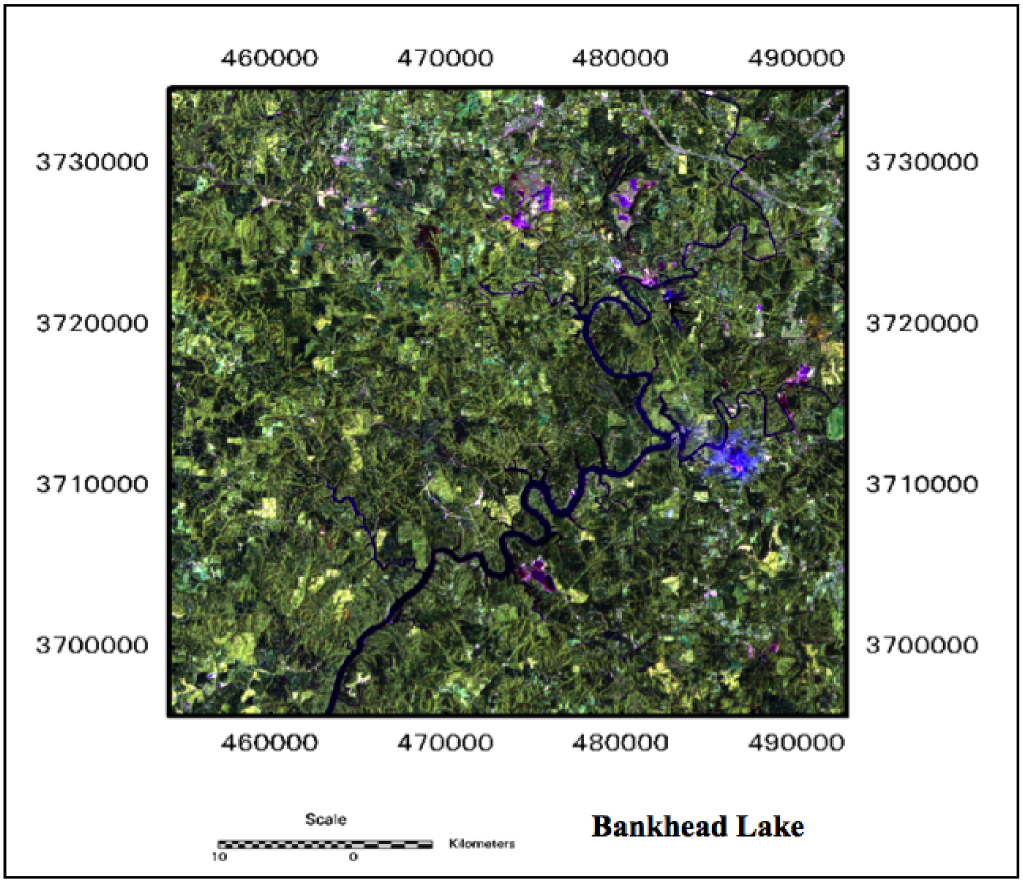

Fig. 1 Landsat TM image displaying Bankhead Lake and surrounding 5 sub-watersheds

Bankhead Reservoir is a man-made lake impounded by the John Hollis Bankhead Lock and Dam and is located approximately thirty miles northeast of Tuscaloosa County covering an area of 9,200 surface acres (ADEM 2004b). A 6,387 km^{2}area drains into Bankhead Reservoir including portions of the Upper Black Warrior, Locust Fork, and Mulberry Fork watersheds of the Black Warrior River Basin (ADEM 2004b). The Mulberry and Locust Forks input into the northern part of the reservoir although the majority of Bankhead Reservoir is located within the Upper Black Warrior watershed. The study area includes Bankhead Reservoir and the surrounding five sub-watersheds seen in Figure 1. Table 2 lists the sub-watersheds that input directly into Bankhead Reservoir and thus were included within the study area. Water samples were taken from the main stem of the lower mid-reservoir; Figure 2 is a map displaying the sample location

Table 2 Five sub-watersheds inputting directly into Bankhead Reservoir

HUC12	Name	Acres	Km^2
31601120202	Lower Big Yellow Creek	13013.1828	52.5867
31601120203	Shoal Creek	52176.3616	210.441
31601120106	Lower Valley Creek	15270.79177	62.5003
31601110413	Coal Creek	22772.8343	92.2397
31601090604	Baker Creek	37027.21819	149.0157

The study area is located within the Cumberland Plateau section of the physiographic province of the Appalachian Plateaus (Fenneman 1938). The geology of this region is made primarily of the Pennsylvanian Pottsville formation characterized by quartzose sandstone and contains varying levels of interstratified dark-gray shale, siltstone, and thin discontinuous coal (Szabo 1988). The topography of this region is severely dissected and no longer resembles a plateau, consisting of narrow ridges and valleys, extensive hills, and steep slopes (USDA 1982). Soils found within this area are acidic, well-drained, and shallow originating from the Muskingum and Pottsville series (USDA 1982).

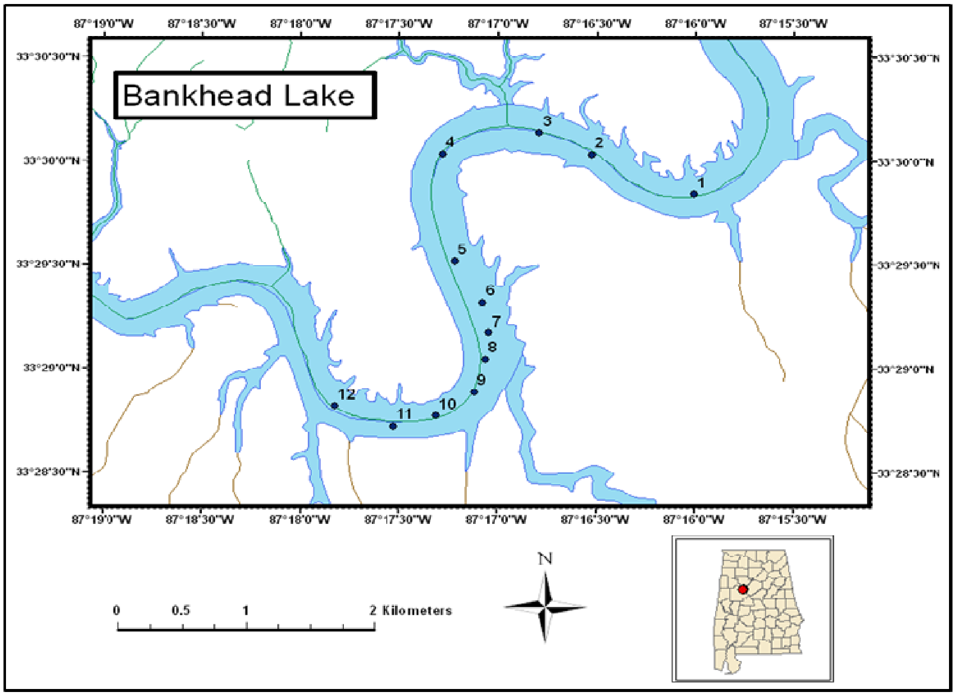

Fig. 2 Map displaying 12 sampling locations in Bankhead's lower mid-reservoir

The climate of this region is classified as humid mesothermal and has short, mild winters and long, hot summers (Thornthwaite 1948). Precipitation is distributed evenly throughout the year, averaging 123 cm annually with means of 12 and 11 cm for January and July (USDA 1982; Smalley 1979). The natural forest cover is made up of oak, hickory, pine, and mixed forest consisting of maple, tuliptree, and linden (Omernick 1987). The Warrior coalfield underlies the study area and though the region is predominately forested ADEM reports that "coal mining is a major industry and the extensive open-pit mines have altered the landscape, soils, and streams" (ADEM 2004c). Shoal Creek Mine is located along and underneath portions of Bankhead Reservoir and discharges wastewater into the mid-reservoir. Several other facilities are permitted to discharge wastewater into the sub-watersheds surrounding Bankhead Reservoir. Table 3 lists the facilities with NPDES permits within the study area.

Table 3 NPDES permits found within the study area

Permit ID #	Permit Name	Major/Minor	Primary Industry Classification (SIC)	Issued	Expiration Date
ALG140263	Quinns Landing INC.	Minor	Marinas	10/1/97	9/30/02
AL0077763	Lost Creek Coalbed methane Pro	Minor	Crude petroleum & Natural gas	3/31/06	3/31/11
AL0068390	El Paso Exploration White Oak	Minor	Crude petroleum & Natural gas	10/10/08	10/9/13
ALG670039	Enterprize AL Jefferson Co	Minor	Natural gas transmission	9/28/07	9/30/12
AL0062421	Drummond Co Inc Shoal Creek	Major	Bituminous coal& Lig, surface	6/22/07	5/31/12
ALG340392	Mikes waste oil service	Minor	Local trucking with storage	1/30/07	1/31/12
ALG360001	Alabama power Co Bankhead Hydr	Minor	Electric services	8/10/04	9/30/09
AL0003387	Drummond Co Mary Lee mine	Minor	Bituminous coal & Lig, surface	2/27/04	4/30/09
AL0002909	Al power Co Gorgas Steam plant	Major	Electric Services	9/6/07	9/5/12
AL0025551	APC Gorgas barge loading facility	Minor	Marine Cargo Handling	9/30/08	9/30/13
AL0026531	Drummond Co Mary Lee mine 2	Minor	Bituminous coal & Lig, surface	9/30/03	9/30/08
AL0066842	New action coal Aldridge mine	Minor	Bituminous coal & Lig, surface	1/30/04	4/30/09
ALG110406	Ready mix USA Quinton plant	Minor	Ready Mix Concrete	8/9/07	8/31/12
ALG110410	Sherman Ind. Inc. Miller	Minor	Ready Mix Concrete	8/7/07	8/31/12
AL0076538	Quinton mining Quinton mine	Minor	No Classifiable Establishment	7/9/04	6/30/09
AL0073717	Gen Power Kelley LLC	Minor	Electrical Services	2/15/06	2/28/11
AL0060305	Swasher #1	Minor	Bituminous coal & Lig, surface	6/22/07	5/31/12
AL0071994	Bessemer Water facility plant	Minor	Water supply	1/20/09	1/31/14
ALG340588	Henery W Head Heads Grocery	Minor	Gasoline service stations	11/17/08	1/31/12
AL0052876	Warrior River WTP	Minor	Water supply	8/27/08	8/31/13
AL0045560	Donaldson Correction Facility AL Utility	Minor	Correctional Institutions	12/21/05	12/31/10
AL0066621	SAGA Petroleum LLC The Narrows	Minor	Crude petroleum & Natural gas	8/31/05	8/31/10

3.2 Collecting and analyzing in situ *data*

Twelve sample sites were established on the main-stem near the middle of Bankhead Reservoir both up and downstream of Shoal Creek Mine (Figure 2). A GPS receiver was used in a boat to locate each sample site for collection of water samples; table 4 lists the geographical locations of twelve sites. Twelve water quality samples were taken to sufficiently estimate a water body of this size. Two sets of ground reference data consisting of TSS and chlorophyll-*a* were collected nearly coincident with the sensor overpass.

Table 4 Geographical locations of 12 sampling sites

Sample	UTM Northing (m)	Latitude	UTM Easting (m)	Longtitude	Average Depth (ft)
1	3706460.38	33.497375	475222.20	-87.266750	51.0
2	3706811.63	33.500521	474409.77	-87.275524	55.5
3	3707004.56	33.502253	474005.09	-87.279868	45.0
4	3706819.60	33.500565	473250.40	-87.287991	70.0
5	3705867.93	33.491981	473344.17	-87.286950	66.5
6	3705499.02	33.488667	473561.22	-87.286404	68.0
7	3705225.60	33.486197	473609.51	-87.284079	69.0
8	3704991.09	33.484086	473583.77	-87.284352	71.5
9	3704696.88	33.481423	473491.05	-87.285333	61.0
10	3704488.18	33.479539	473190.99	-87.288567	73.0
11	3704397.50	33.478710	472861.10	-87.292105	74.0
12	3704574.32	33.480295	472391.56	-87.297169	72.5

Water samples were collected on 28 March 2011 and 18 August 2011. At each site, a 1000 mL water sample was collected approximately one foot below the water's surface. To prevent the deterioration of algae and other organic matter, the sample bottles were kept in an ice cooler until analyzed in the lab for chlorophyll-*a* and TSS concentrations.

3.2.1 March Sampling Conditions

The first set of water samples were scheduled to be collected in early March; however due to the Landsat TM image overpass and image availability the water samples were collected in late March. The late winter/early spring time of year was chosen for sampling because it is before deciduous plant species have fully re-vegetated therefore increasing the rate of erosion into streams and Bankhead Reservoir. Water samples were collected from all twelve sites between 1:00 and 3:00 P.M. on 28 March 2011. It was partly overcast with a temperature in the mid-60s and a slight wind coming from the SE. The USGS station 02462500 at Bankhead Lock and Dam (33.4583 °N, 87.3542 ° W), located approximately 14.5 km downstream of sample locations, recorded 1.76 in. (4.47 cm) of rain during the two weeks prior to collection (figure 3). This station no longer records discharge rates and data from USGS station 02456500 on the Locust Fork (33,4472° N, 87.1222° W) was used for discharge comparison. The Locust Fork inputs into Bankhead approximately 16 km upstream from sample locations and was discharging 3,040 ft^{3}s^{-1} (926.6 m^{3}s^{-1}) during collection. Figure 3 shows the hydrograph for USGS station 02456500 at the Locust Fork from 01 January to 01 May 2011. On the sampling day, discharge was over 1000 ft^{3}s^{-1} (305 m^{3}s^{-1}) greater than the median daily average due to precipitation from a small frontal storm that moved through the study area. According to the hydrograph, samples were collected when discharge was slightly elevated. However, it was significantly below flood stage that discharges at almost 20,000 ft^{3}s^{-1}.

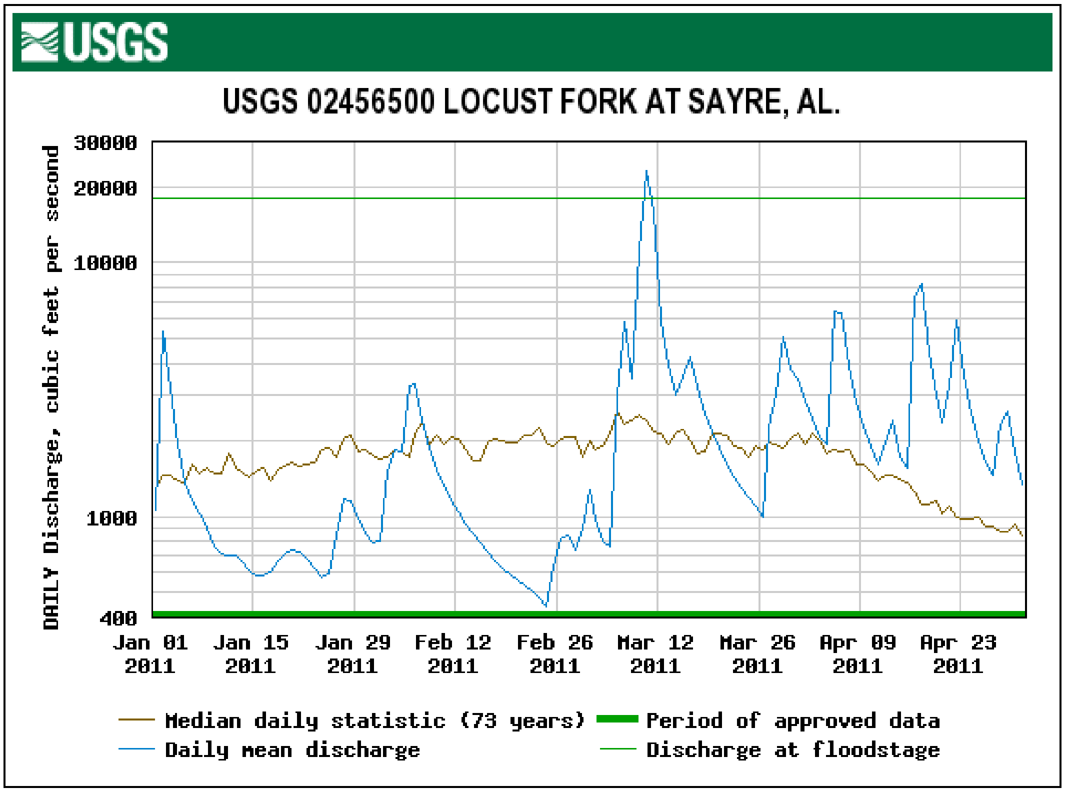

Fig. 3 Discharge hydrograph during March sampling conditions

3.2.2 August Sampling Conditions

Water samples were collected in August when chlorophyll-*a* levels are at their most critical levels for management. The specific date for sampling was determined based on the Landsat TM sensor overpass. Water samples were collected from all twelve sites between 10:00 and 12:00 P.M. on 18 August 2011. Weather conditions were mostly sunny with temperatures in the mid-90s and a slight wind coming from the NW. The USGS station 02462500 at Bankhead Lock and Dam recorded 2.37 in. (6.02 cm.) of rain during the two weeks prior to collection. Figure 4 shows the hydrograph for USGS station 02456500 at the Locust Fork from 01 January to 01 October 2011. The Locust Fork was discharging 84 ft^3s^{-1} (25.6 m^3s^{-1}) on the day of August sample collection. On the sampling day, discharge was 50 ft^3s^{-1} (15.2 m^3s^{-1}) below the median daily average. According to the hydrograph, samples were collected when discharge was at significantly low-flow.

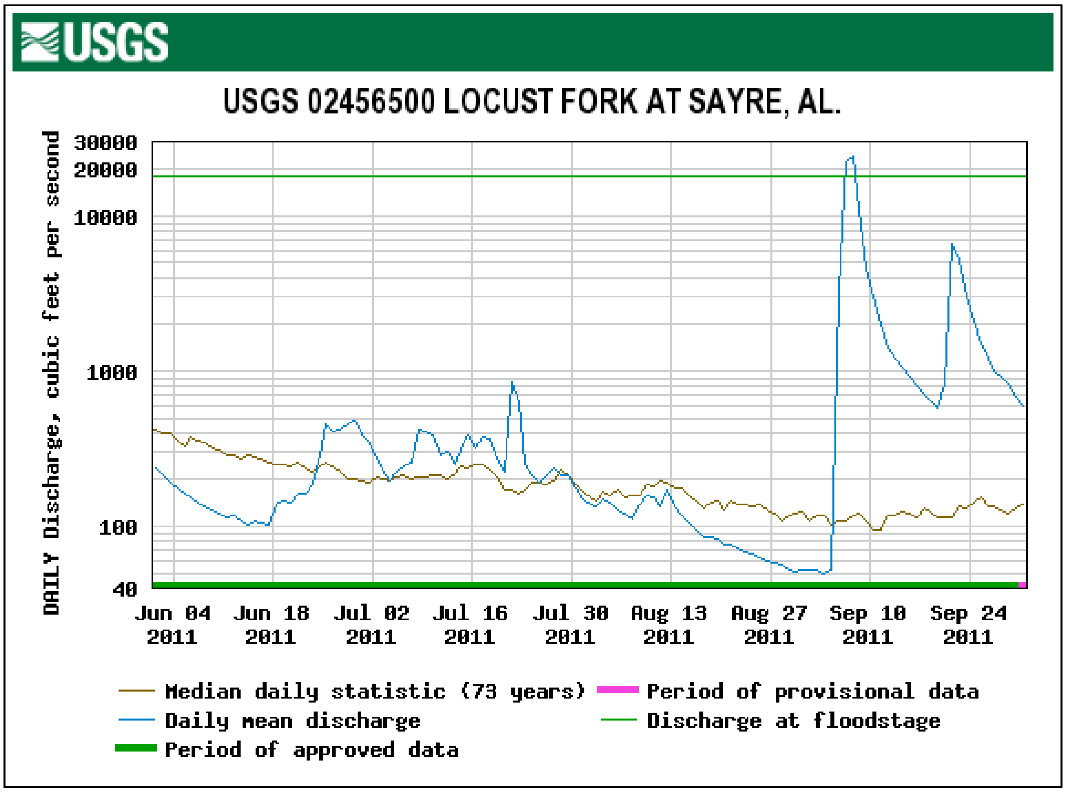

Fig. 4 Discharge and precipitation hydrographs during August sampling conditions

3.2.3 Lab analysis

The University of Alabama's Aquatic Biology Lab analyzed the water samples. Two different procedures were used to calculate TSS and chlorophyll-*a* concentrations. Each sample was divided into two sub-samples for the different procedures. Dividing a sample into subsamples can introduce error into the analysis and must be considered when analyzing the results (Glysson *et al.* 2000). Total suspended solids were analyzed according to a procedure provided by the *Standard Methods for the Examination of Water and Wastewater* (APHA 1992). First a well-mixed sample was filtered through a standard, pre-weighed, glass-fiber filter. The remaining residue was then dried to a constant weight at 103-105□C. The increase in the filter's weight indicates the amount of total suspended solids.

The remaining sub-samples were analyzed for chlorophyll-*a* according to the EPA Method 445.0 (Arar and Collins 1997). This procedure can determine the chlorophyll-*a* in both marine and freshwater phytoplankton by using fluorescence detection (Arar and Collins 1997). Each sub-sample was first concentrated by filtering with a low vacuum through a fiber filter. The filters were then torn into small strips and incubated for eighteen hours in 90% acetone in the freezer and subsequently vortexed at several intervals (NSF 2004). This part of the method followed the Natural Science Foundation's Long Term Ecological Research Site procedures used at the Toolik Field Station in Alaska. The EPA method was used with the exception of this step. To clarify the solution, the filter slurry was centrifuged at 675 g for fifteen minutes. The fluorescence of an aliquot was then measured before and after acidification to 0.003 N HCL, by adding 0.1 N HCL. Finally, sensitivity calibration factors were used to calculate the concentration of chlorophyll-*a* in the sample extract (Arar and Collins 1997).

3.3 Remotely sensed data processing

The remotely sensed data used for this study includes two Landsat-5 TM images (path: 21 and row: 37) acquired on 25 March 2011(ID: LT50210372011084GNC01) and 16 August 2011 (ID: LT50210372011228GNC01). The images were downloaded from the USGS Global Visualization Viewer (GloVis), an online search and order tool for free satellite data. The March image contains a small patch of smoke minimally impacting Locust Fork of the Black Warrior River; the August image contains small pockets of clouds, but Bankhead Reservoir had minimal cloud cover. No sample locations in the lake were impacted. ERDAS Imagine is the digital image processing software used to process the Landsat TM data. Each image was first subset to the much smaller study area to ease in the selection of ground control points (GCP) used in geometric correction. Figure 5 displays both the original Landsat TM March and August scenes downloaded from USGS as well as the study area subset images. Twenty-four ground control points were selected from the images and rectified to the UTM (Universal Transverse Mercator) WGS 84 projection using coordinates obtained from Google Earth. Previous studies have proven twenty-four GCP's to be sufficient in geometric correction. For the spatial interpolation of the geometric correction, a first-order polynomial transformation was used and the RSME was less than 0.5 pixel. The image's original digital numbers (DNs) were preserved by subsequently using a nearest-neighbor resampling method. Figure 5 displays both March and August Landsat full scenes and study area subsets as false color composite images; note the vegetation (red) difference from March to August. In March, before vegetation has had time to reach its growth peak, the land use difference within the study area is more clearly displayed. The March image was also less impacted by clouds and thus chosen for later use in image classification.

After geometric correction, the images were atmospherically corrected. The atmosphere may potentially affect an image by absorbing, scattering and refracting light (Chavez 1988). Atmospheric correction is carried out to minimize these atmospheric effects and convert digital numbers (DNs) to at-sensor reflectance values (Moran *et al.* 1992; Chavez 1996). Atmospheric correction methods that use ground-truth information are the most accurate and generally preferable, but are difficult to implement and the necessary input data is not always readily available (Chavez 1988, 1996). Chavez (1996) found that the entirely image-based COST model to be as accurate as models using ground truth atmospheric field measurements. An adaptation of the Chavez (1996) COST model was used in order to minimize atmospheric effects. An excel spreadsheet and Erdas Spatial Model was implemented to convert digital numbers (DNs) to at-sensor reflectance values (Skirvin 2000). The general radiance to reflectance equation (Chavez 1996) implemented was:

$$R = \pi * d^2 * (L_{\lambda sat} - L_{\lambda haze})/ESUN_\lambda * \cos^2\theta \qquad (1)$$

The model inputs include Earth-Sun distance, sun elevation angle, and the minimum DNs for bands 1-5 and 7. The model output is in reflectance units with image values ranging from 0 to 1.

Following atmospheric and radiometric correction, a land-masked image was produced to black out land pixels for the purpose of creating images that can be processed to enhance water features only. Band 4 was utilized to differentiate between land and water surfaces. The band 4 raster layer was studied and a threshold value was determined for each image (March = 0.34; August = 0.36); values below the threshold are water pixels and above the threshold are land pixels. A simple spatial model was created in Erdas Imagine to mask land pixels based on band 4 values. The model recoded all band 4 reflectance values below the threshold to 1 (water pixels) and all values above the threshold to zero (land pixels). A recoded image with water pixels equal to 1 and land pixels equal to zero was produced and multiplied with the original image to create a land-masked image containing water pixel reflectance values only.

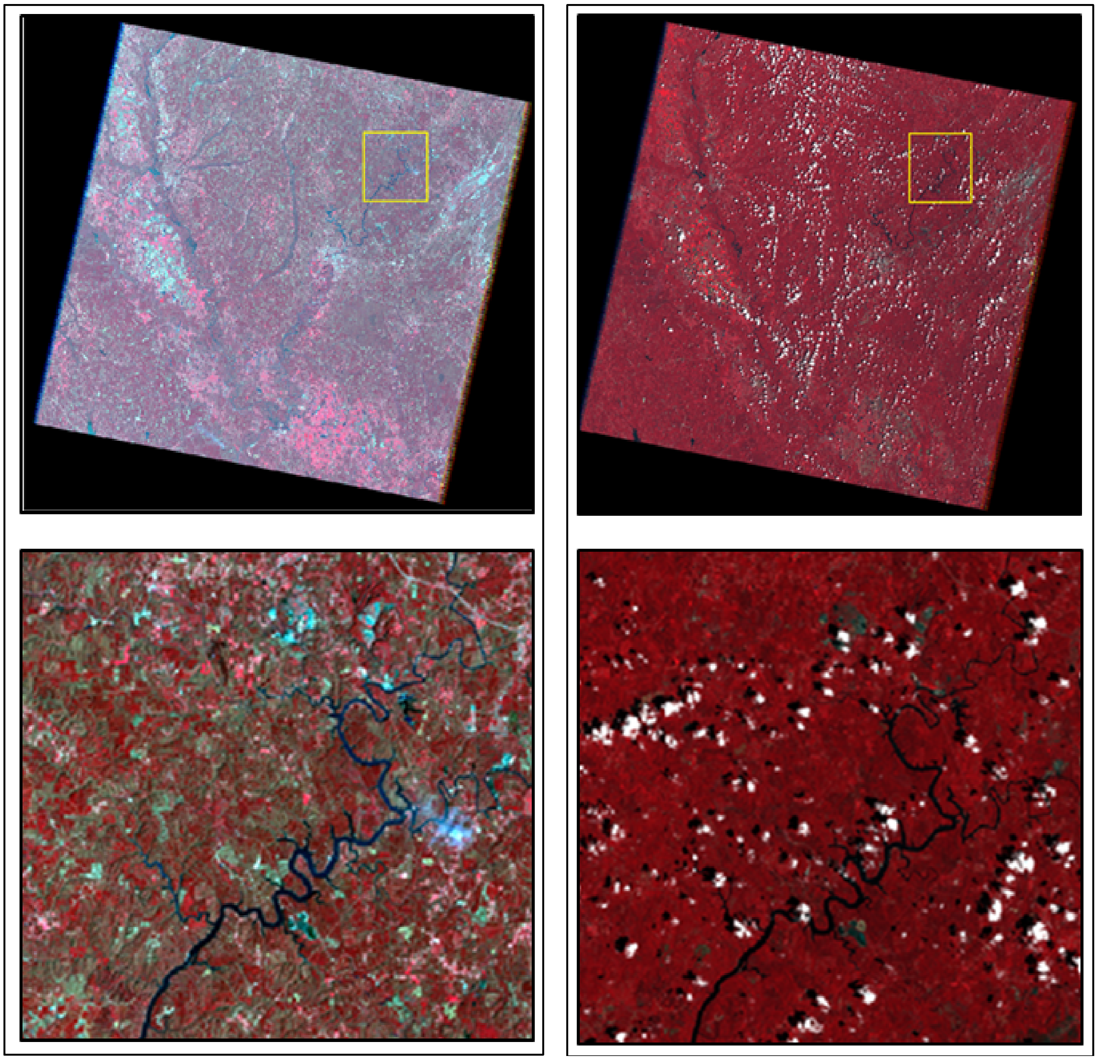

Fig. 5 March (left) and August (right) Landsat TM full scenes (top) and study area subsets (bottom)

3.4 Creating land use/land cover map using supervised image classification

It is well known to hydrologists that water quality is significantly impacted by the surface cover water travels over into receiving streams or lakes (Zhang and Wang 2012). Water quality is influenced by land use because it determines the type and amount of nonpoint source pollutants that could enter the watershed (Zhang and Wang 2012). Consequently, the land use-land cover in a watershed will affect water quality and nonpoint source pollution is an increasing environmental concern (Griffith 2002). A land use/land cover map was created using supervised image classification in Erdas Imagine to briefly explore the potential causes of water quality variation. The March image was chosen due to less cloud cover and less vegetation, which eased in differentiating between land use types. In supervised classification the user defines the training data, or spectral signature, which tells the software the type of pixels to choose for certain land use types. Knowledge of the study area, Google Earth satellite imagery, and previous experience in image interpretation eased supervised classification of the study area image.

The March 2011 Landsat image was used for classification and included smoke that impacted a small section of the Locust Fork near Bankhead Reservoir. The following classes were used in image classification: water, coniferous, deciduous, open-field, low-intensity development, and high-intensity development. The water class includes Bankhead Reservoir, the Mulberry and Locust Forks, and the upper end of Holt Reservoir. The forest surrounding Bankhead contained both coniferous and deciduous tree species. The coniferous forest is made up of loblolly-shortleaf pine and the deciduous forest consists of both oak and hickory species (AFC 2010). The open-field class includes areas that have no trees and are grassy or partially grassy. Primarily abandoned mining grounds make up the open-field class within the study area. Low-intensity development includes areas consisting of both constructed materials and vegetation. High-intensity development contains commercial areas with impervious surfaces and/or significantly disturbed land. The smoke class is included on the map but was manually imposed after classification.

To ensure the accuracy of the classification, an accuracy assessment on the Land Use/Land Cover map was used to compare certain pixels in classified subsets to reference pixels. The exercise was implemented from the ERDAS tour guide. The thirty reference pixels used were known using ground truth data, Landsat TM imagery, and Google Earth. The Kappa coefficient, in the results of the accuracy assessment displays the proportionate decrease in error produced in a classification process compared to the error of a random classification. The map created had a Kappa coefficient of 0.80 indicating that the classification successfully avoided 80% of the errors that a totally random classification would produce (Congalton 1991).

3.5 Relationship between reflectance and water quality parameters

The geometrically and atmospherically corrected land masked Landsat TM images were used for water quality spatial analysis in this study. The twelve sampling points were located on the image based on the UTM coordinates determined with a GPS during water sampling and extracted for use in correlation and regression modeling. Only the single pixel value for each sampling location was extracted. Several previous studies have instead extracted a 3x3 window around each sampling pixel to improve the signal-to-noise ratio as well as compensate for coordinate disparity errors (Brivio *et al*. 2001; Wang *et al*. 2005; Zhou *et al*. 2006). However, in this particular study the single pixel extraction method was preferred due to the narrowness of the reservoir. Using a 3x3 pixel window for each sampling point may include shallower water near the banks of the reservoir that could potentially alter reflectance values.

A Pearson correlation matrix was first developed to determine the strengths of correlation between water quality concentrations and TM bands and band ratios. Linear and quadratic polynomial regression methods were subsequently used to further explore the relationship between water quality parameters and spectral reflectance. TM bands 1-4 reflectance values at each sample site were extracted from both images for use as independent variables in bivariate regression models. Only the first four TM bands were used for this analysis based on examination of the data and the study by Dekker and Peters proving other bands provide little water quality information (1993). Independent variables include: TM1, TM2, TM3, TM4, TM1/TM2 (R12), TM1/TM3 (R13), TM1/TM4 (R14), TM2/TM3 (R23), TM2/TM4 (R24), TM3/TM34 (R34). Dependent variables that were analyzed include total suspended solids, logarithmically transformed total suspended solids, chlorophyll-*a*, and logarithmically transformed chlorophyll-*a*. SPSS was used for the statistical analysis required in this study. Regression models were chosen to estimate both TSS and chlorophyll-*a* in Bankhead Reservoir based on correlation coefficients, standard error of estimate (SEE), actual vs. predicted water quality values and visual interpretation of the maps produced. The regression equations believed to be the most successful were implemented to map the TSS and chlorophyll-*a* concentrations in Bankhead Reservoir.

4. Results and discussion

4.1 Land Use/Land Cover map

The Land Use/Land Cover map includes Bankhead Reservoir and the neighboring five sub-watersheds (Figure 6). The study area surrounding Bankhead Reservoir consists of mostly mixed forest (66.7%) and low-intensity development (26.2%). Interstate- 22 is clearly displayed in the northeast section of the map separating the towns of Sumiton on the east from the Oakman, Parrish, and Good Springs on the west. The edge of Hueytown, a western suburb of Birmingham, is found on the southeastern corner of the study area map. Smoke can be seen near the Locust Fork.

Table 5 Percent surface cover and square kilometers of land use within study area

Land Use	km^2	% Cover
Water	23.30	1.76
Coniferous Forest	294.74	22.32
Deciduous Forest	586.74	44.43
Open-field	0.53	0.39
High-intensity development	63.78	4.83
Low-Intensity development	346.51	26.24

Table 5 lists the total (km^2) and percent land cover for land use types within the study area. The towns found within the study area are mostly low-intensity development and cover 26% of the surface cover; small towns can be significant contributors of nonpoint source pollution. Urbanized areas have a greater amount of impervious surfaces and can increase the amount of runoff introducing elevated nutrient and sediment loads into the watershed (Emmerth and Bayne, 1996; Wahl *et al.*1997). The high-intensity development within the study area consists mostly of surface and underground coalmines and coal bed methane mines. Alabama Power’s Miller Steam Plant is found on the Locust Fork of the Black Warrior River and is classified on the map as high-intensity development due to mining and waste disposal infrastructure. Alabama Power’s Gorgas Steam Plant is found on the Mulberry Fork of the Black

Warrior River and is also classified as high-intensity development. Shoal Creek Mine is clearly displayed as high-intensity development inputting into Bankhead's mid-reservoir. Shoal Creek Mine is high-intensity because mining operations have completely altered the surface of the earth impacting hydrologic and ecologic systems. High-intensity development found within the study area is only 4.8% of the land cover. The open fields found within the study area are mostly abandoned mining areas, which increase erosion and sedimentation during precipitation events. Open fields have the smallest surface cover and are only 0.39% of the study area. The forest surrounding Bankhead Reservoir is composed of mostly deciduous trees (44%) with a smaller amount of coniferous trees (22%) as well.

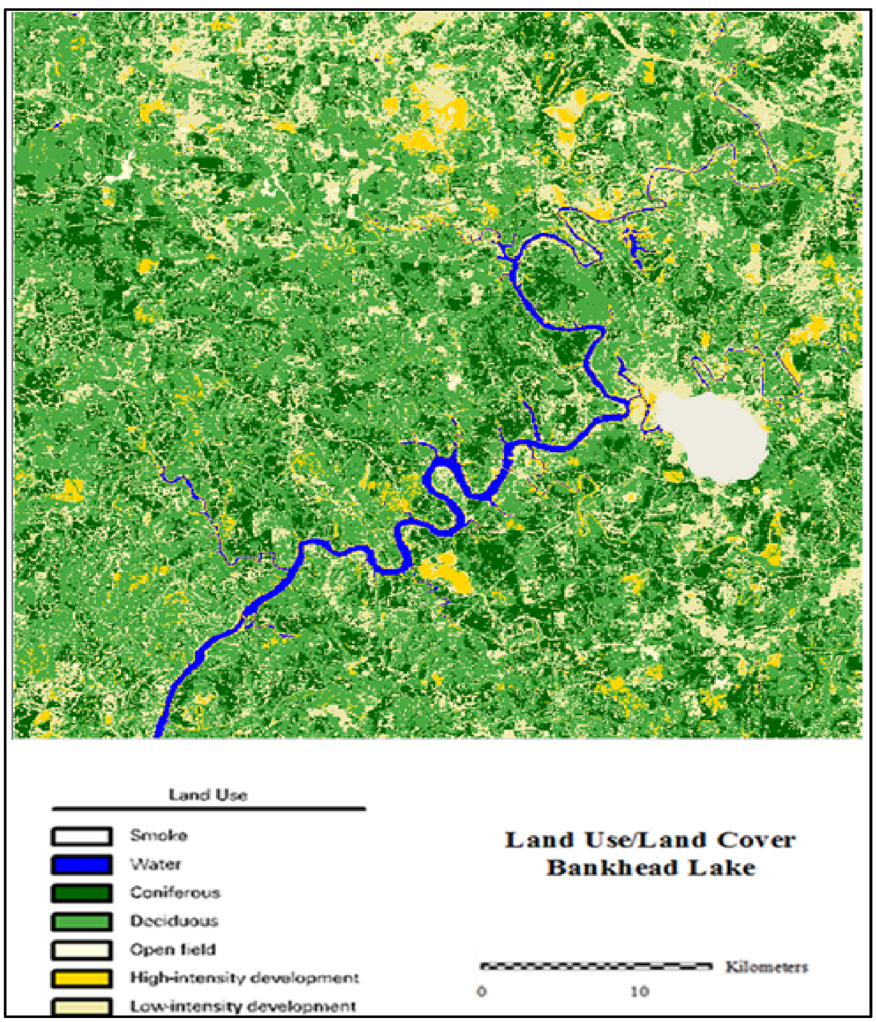

Fig. 6 Land Use/ Land Cover Map of Bankhead Lake

4.2 March data

4.2.1 In-situ water quality data

Table 6 March lab-measured TSS, chlorophyll-*a*, and SDD values

Sample	TSS (μgl^{-1})	Chlor-*a* (μgl^{-1})
1	3.38	9.47
2	4.72	6.56
3	4.90	9.38
4	4.86	9.40
5	4.66	10.14
6	4.41	10.26
7	4.57	8.83
8	5.02	8.50
9	4.36	7.62
10	4.39	8.65
11	4.15	9.13
12	4.12	8.21

Table 6 shows the laboratory-measured total suspended solids and chlorophyll-*a* concentrations found at the twelve sampling sites. The mean TSS was 4.50 $mg1^{-1}$ and had a standard deviation of 0.45 mgl^{-1} indicating a low spatial variability of TSS in the mid- reservoir (table 7). The river's discharge was slightly higher than the 73-year average daily mean discharge as a result of a small frontal system that moved through the study area during 26-28 March 2011, but was still significantly below discharge at flood stage. The highest amount of TSS (5.02 mgl^{-1}) was recorded at site eight near the barge loading area of Shoal Creek Mine's processing plant loading facility. TSS levels were expected to be slightly higher and more variable because at the time of sampling vegetation was not fully leafed out which should increase TSS into surface waters. The mean chlorophyll-*a* concentration was 8.85 μgl^{-1} and had a standard deviation of 1.05 μgl^{-1}. The highest amounts of chlorophyll-*a* were found at sites five and six and the lowest concentration was found at site two. Chlorophyll-*a* levels were relatively low as expected for this time of year because vegetation has not fully bloomed and conditions are not favorable for algae growth.

Table 7 Descriptive statistics for March water quality data

Parameter	N	Minimum	Maximum	Mean	Std. Deviation
Total Suspended Solids (mgl^{-1})	12	3.38	5.02	4.46	0.45
Chlorophyll-*a* (μgl^{-1})	12	6.56	10.26	8.85	1.05

4.2.2 Correlating water quality and reflectance

Statistical techniques were used to derive correlations between TM bands 1-4 spectral reflectance data and TSS and chlorophyll-*a*. Table 8 shows the pixel reflectance for each sampling location extracted from the March Landsat TM image. To examine the relationship between water quality parameters and TM bands and band ratios during both March and August conditions, a Pearson correlation and regression analysis was performed separately on each dataset. A Pearson correlation matrix was developed to determine the strengths of correlation between water quality parameters and TM bands and band ratios. Table 9 lists the correlation coefficients between March TSS and chlorophyll-*a* concentrations and TM bands and band ratios utilized in this study. The strengths of correlation between bands and band ratios differ for each water quality parameter.

Table 8 TM bands 1-4 reflectance for each sampling site

Sample	TM Band 1	TM Band 2	TM Band 3	TM Band 4
1	0.022	0.020	0.013	0.014
2	0.018	0.020	0.016	0.010
3	0.020	0.020	0.016	0.014
4	0.020	0.024	0.016	0.014
5	0.018	0.020	0.016	0.018
6	0.018	0.024	0.013	0.014
7	0.018	0.020	0.016	0.014
8	0.018	0.020	0.016	0.010
9	0.018	0.020	0.013	0.010
10	0.018	0.020	0.016	0.010
11	0.017	0.024	0.013	0.014
12	0.018	0.020	0.013	0.010

Band 3 has the strongest single band correlation with TSS, but band ratio R1/3 was found to have the strongest overall relationship to TSS concentrations found in Bankhead Reservoir. TSS is positively correlated with TM 3 and negatively correlated with ratio R1/3. This supports other findings that reflectance increases in the red region of the visible spectrum as suspended sediment concentration increases (Han 1997; Novo *et al.* 1991). The increase in band 3 with increased TSS concentration causes R13 to have a negative correlation with TSS; as TSS increases, R13 decreases.

Chlorophyll-*a* was most highly correlated with TM Band 4 and band ratios R1/3, R2/4 and R3/4. Algal-laden waters have a distinct spectral curve with absorption in the blue region, maximum reflectance in the green region, absorption in the red region, and a reflectance peak at the red/NIR spectral boundary (Han 1997). Band 4 is most likely significantly correlated with chlorophyll-*a* because band 4 brightness values are responding to the peak in NIR reflectance as a result of increased algae in the water. R1/4 has a strong negative correlation with chlorophyll-a; band 4 reflectance steadily increases with increased chlorophyll concentration causing R1/4 to have an overall negative relationship with chlorophyll-*a* concentration. Similarly, band ratio 2/4 also has a negative relationship with chlorophyll-*a*.

4.2.3 Estimating TSS in Bankhead Reservoir during March conditions

Table 9 Pearson correlation coefficients between water quality parameters and various Landsat TM band and band ratios

		TM 1	TM 2	TM 3	TM 4	R1/2	R1/3	R1/4	R2/3	R2/4	R3/4
Total Suspended Solids	r	-0.27	0.02	**0.75**	-0.03	-0.22	**-0.81**	-0.01	-0.52	0.08	0.37
	Sig. *	0.39	0.95	**0.01**	0.93	0.50	**0.00**	0.97	0.09	0.81	0.24
Chlorophyll-*a*	r	0.24	0.43	-0.08	**0.80**	-0.12	0.20	**-0.77**	0.29	**-0.73**	**0.77**
	Sig.*	0.46	0.16	0.81	**0.00**	0.70	0.54	**0.00**	0.36	**0.01**	**0.00**

Reflectance values were used in building both single band and band ratio regression models to estimate TSS concentrations. Linear bivariate models were first established using single band reflectance and logarithmically transformed reflectance as independent variables and TSS and logarithmically-transformed TSS as dependent variables (Chang 2004; Zhou *et al*. 2006). Table 10 lists the R^2 and standard error of estimate (SEE) for single band models and TSS concentrations. TM 3 was the only single band with a significant relationship with TSS regardless of the model type chosen. These findings are consistent with several previous investigations that concluded TM 3 has the strongest relationship with suspended matter or suspended sediments in surface water (Dekker *et al*. 2002; Lathrop 1992; Nas *et al.* 2010; Ritchie *et al.* 1987; Zhou *et al*. 2006).

Table 10 R^2 and **SEE (mgl^{-1})** for single band models

TSS Regression Models	TM 1	TM 2	TM 3	TM 4
$tss = y_0 + a * b_j$	0.08 **(0.45)**	0.00 **(0.47)**	0.56 **(0.31)**	0.00 **(0.47)**
$tss = y_0 + a * \log(b_j)$	0.06 **(0.45)**	0.00 **(0.47)**	0.56 **(0.31)**	0.00 **(0.47)**
$\log(tss) = y_0 + a * b_j$	0.11 **(1.12)**	0.00 **(1.12)**	0.53 **(1.08)**	0.00 **(1.12)**
$\log(tss) = y_0 + a * \log(bj)$	0.09 **(1.12)**	0.19 **(9.75)**	0.53 **(1.08)**	0.00 **(1.12)**

The second type of bivariate linear model was established using band ratio reflectance and logarithmically transformed ratio reflectance as independent variables; TSS and logarithmically transformed TSS as dependent variables. Table 11 lists the R^2 and SEE for band ratio models and TSS concentrations. R13 was the only single band with a significant relationship with TSS concentration regardless of the model type chosen. A study by Lathrop found that band ratios consisting of longer wavelength bands TM2 and TM 3 over shorter wavelength band TM 1 have a significant positive relationship with suspended solids (1992). Similar findings by Nas *et al*. (2010) found a relationship exists between suspended solids and R3/1. In this study, R1/3 has a significant relationship because reflectance in the red region (TM3) increases faster than in the blue region (TM1). Ratios of shorter wavelengths over longer wavelengths have a negative relationship.

Table 11 R^2 and **SEE (μgl^{-1})** for band ratio models estimating TSS

TSS Regression Models	R1/2	R1/3	R1/4	R2/3	R2/4	R3/4
$tss = y_0 + a * (b_j/b_k)$	0.046 **(0.457)**	0.653 **(0.276)**	0.000 **(0.468)**	0.266 **(0.401)**	0.006 **(0.467)**	0.137 **(0.435)**
$tss = y_0 + a * \log(b_j/b_k)$	0.027 **(0.462)**	0.624 **(0.287)**	0.001 **(0.468)**	0.283 **(0.396)**	0.004 **(0.467)**	0.142 **(0.434)**
$tss = y_0 + a * (\log b_j/\log b_k)$	0.023 **(0.463)**	0.610 **(0.292)**	0.002 **(0.468)**	0.263 **(0.402)**	0.003 **(0.468)**	0.040 **(0.459)**
$\log(tss) = y_0 + a * (b_j/b_k)$	0.007 **(1.114)**	0.675 **(1.067)**	0.000 **(1.119)**	0.242 **(1.102)**	0.009 **(1.117)**	0.137 **(1.109)**
$\log(tss) = y_0 + a * \log(b_j/b_k)$	0.042 **(1.117)**	0.642 **(1.069)**	0.001 **(1.119)**	0.260 **(1.102)**	0.006 **(1.119)**	0.143 **(1.109)**
$\log(tss) = y_0 + a * (\log b_j/\log b_k)$	0.037 **(1.117)**	0.630 **(1.072)**	0.003 **(1.119)**	0.241 **(1.102)**	0.005 **(1.119)**	0.044 **(1.117)**

The single band regression model was chosen to map TSS in Bankhead Reservoir during the spring season and is considered superior to other tested band and band ratio algorithms based on values of correlation coefficients, SEE, actual vs. predicted TSS values and the visual interpretation of maps produced. The single band regression model employed to map TSS concentrations in Bankhead Reservoir during observed spring water quality conditions had the form of:

$$\log(TSS) = y_0 + a * b_j \tag{2}$$

Where TSS is total suspended solids concentration (mgl^{-1}); y_0 is the regression constant; a is the regression coefficient; and b_j is TM band 3.

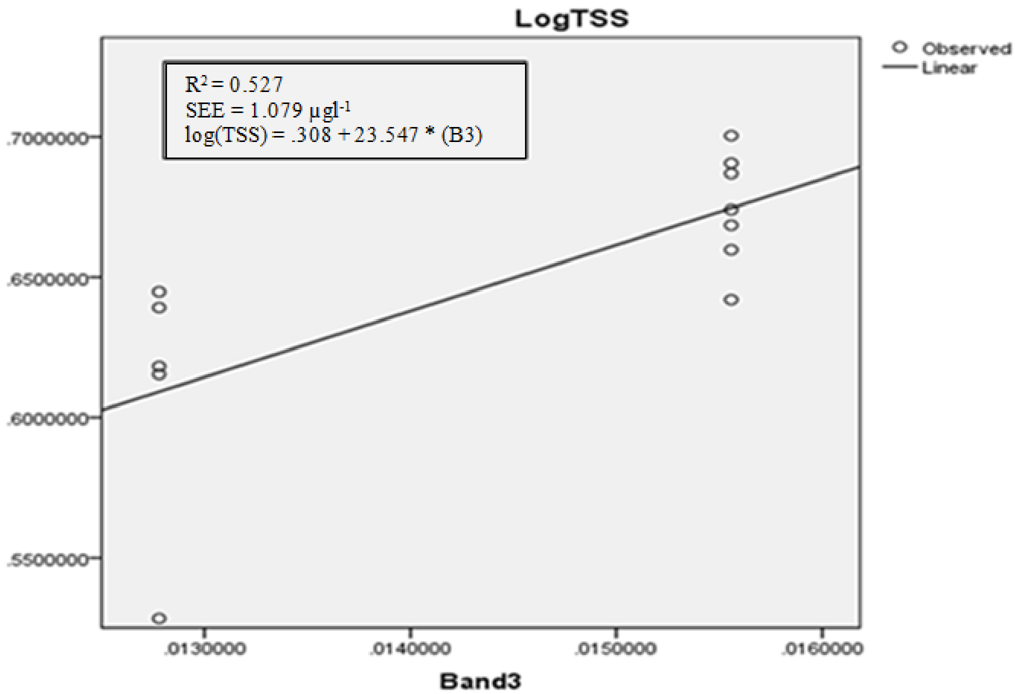

Fig. 7 Statistical results using chosen regression model to estimate March TSS concentrations

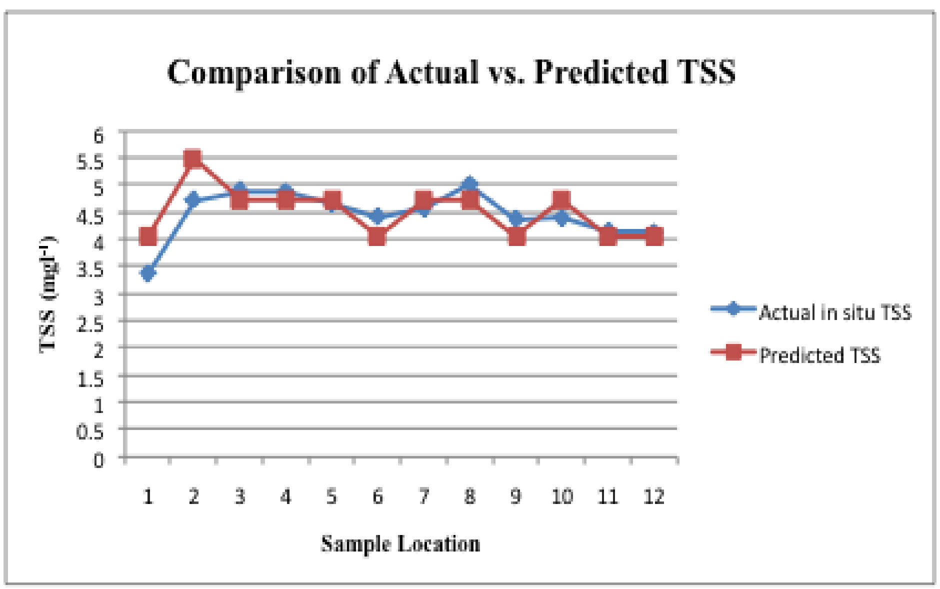

Fig. 8 Comparison of Actual vs. Predicted March TSS concentrations

Figure 7 summarizes the statistical results using the regression model described in equation (2) to estimate TSS. The R^2 value was 0.527 ($p<0.008$) and the SEE was 0.033 (1.079 $mg1^{-1}$). Higher concentrations of total suspended solids increase the reflection in TM band 3 and though the variation in TSS and brightness values is extremely small within this dataset these findings suggest that the Landsat sensor successfully detected the small differences in concentrations. Figure 8 shows the comparison of the estimated TSS with actual *in situ* sample data. The TM3 single band model using equation (2) provides reasonable TM-derived TSS concentrations and has a small SEE of only 1.079 mgl^{-1}. TSS concentrations derived from March Landsat reflectance values were on average slightly higher than the in-situ data.

Using this model, a TSS concentration map was produced using ERDAS imagine software (Figure 9). The map successfully characterizes the spatial pattern of TSS in Bankhead Reservoir of the Black Warrior River. TSS concentrations found in Bankhead Reservoir and its tributary embayment's varied between 1.9 and 18.1 mgl^{-1} during observed March conditions. The water quality map produced indicates that there is a higher abundance of TSS in the upper part of the reservoir and gradually declines moving downstream towards the dam forebay. This indicates that sediment could be settling in the upper part of the reservoir. The upper Mulberry Fork contained some of the highest TSS levels found within the reservoir (11.3 - 18.1 mgl^{-1}). In the Baker Creek sub-watershed of the Mulberry Fork there is significant high-intensity development from surface coal mining and coal-bed methane mining. The Locust Fork was minimally impacted by smoke near where it inputs into Bankhead Reservoir; the upper reaches of Locust Fork were not impacted and have TSS levels between 4.2 - 18.1 mgl^{-1}.

Several tributary embayments that input into Bankhead Reservoir were also mapped during March conditions. Figure 10 contains enlarged image subsets of the major tributaries contributing to Bankhead Reservoir. Big Yellow Creek had the greatest concentrations of TSS of all the tributaries inputting into the reservoir. The Big Yellow Creek embayment had TSS levels varying between 11.31 – 18.10 mgl^{-1} which was significantly higher than the lower main stem of the reservoir, only averaging between 1.94 – 4.20 mgl^{-1}. TSS concentrations in the Big Yellow Creek embayment increased upstream and were the highest of any other tributary. The Lost Creek embayment had TSS levels between 4.20 and 18.10 mgl^{-1} and concentrations increased upstream from Bankhead Reservoir.

TSS levels in Valley Creek were slightly less (4.20 – 11.31 mgl^{-1}) than concentrations found in Lost Creek but similar to levels found in the upper main stem of the reservoir. Little Shoal Creek and Shoal Creek input into the lower mid-reservoir near where water samples were collected. Little Shoal Creek had low TSS levels (1.94– 4.20 mgl^{-1}). The Shoal Creek embayment generally had TSS concentrations similar to Little Shoal Creek; however, portions near the far upper and lower embayment had slightly elevated TSS concentrations (7.1091 – 11.3095 mgl^{-1}). Elevated TSS levels could be due to excess discharges from Shoal Creek Mine resulting from the recent precipitation event. It is important to understand the spatial variation of TSS found in Bankhead Reservoir during late winter/early spring background conditions for comparison in future synoptic studies of the reservoir.

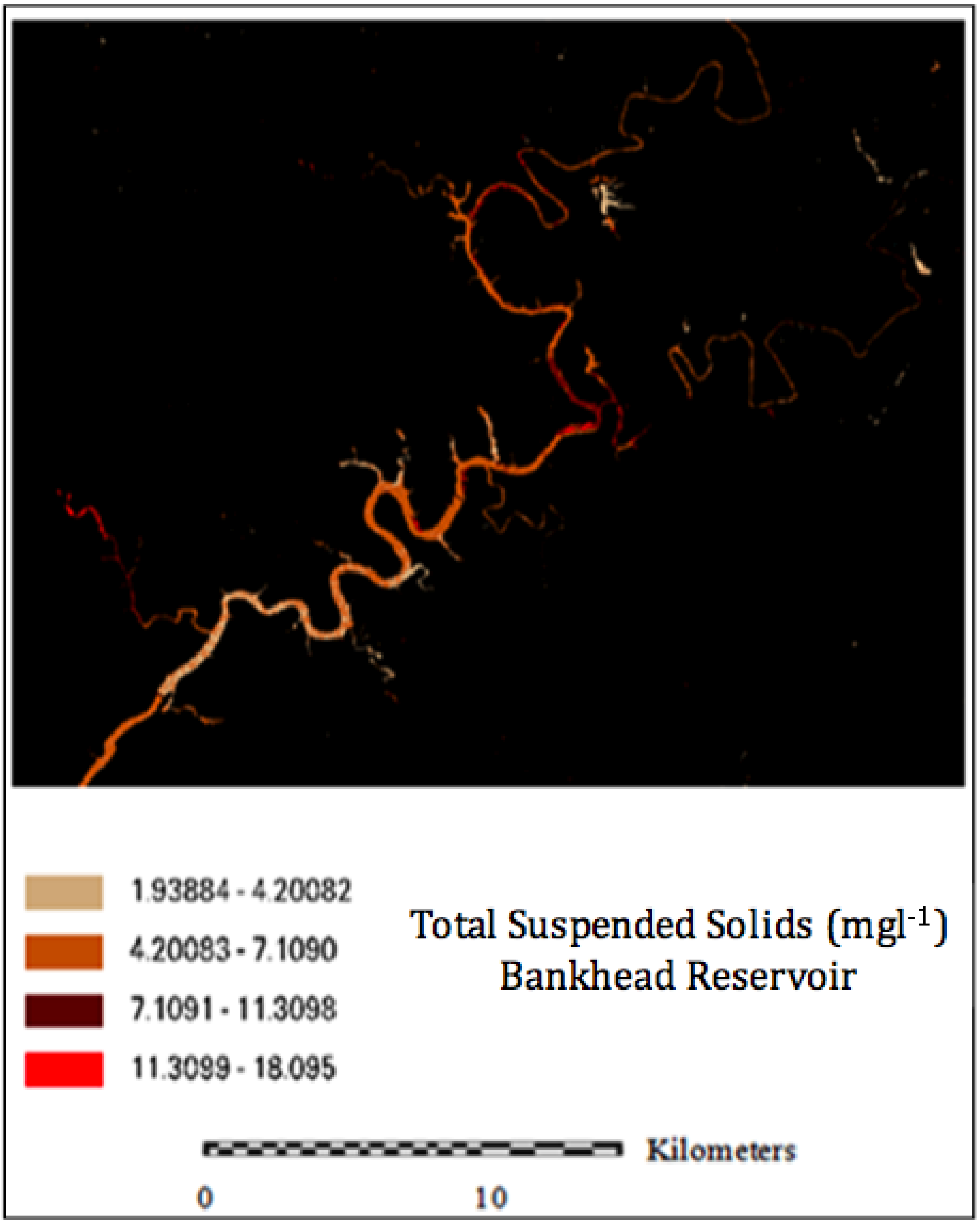

Fig. 9 TSS concentration map of Bankhead Reservoir during March conditions

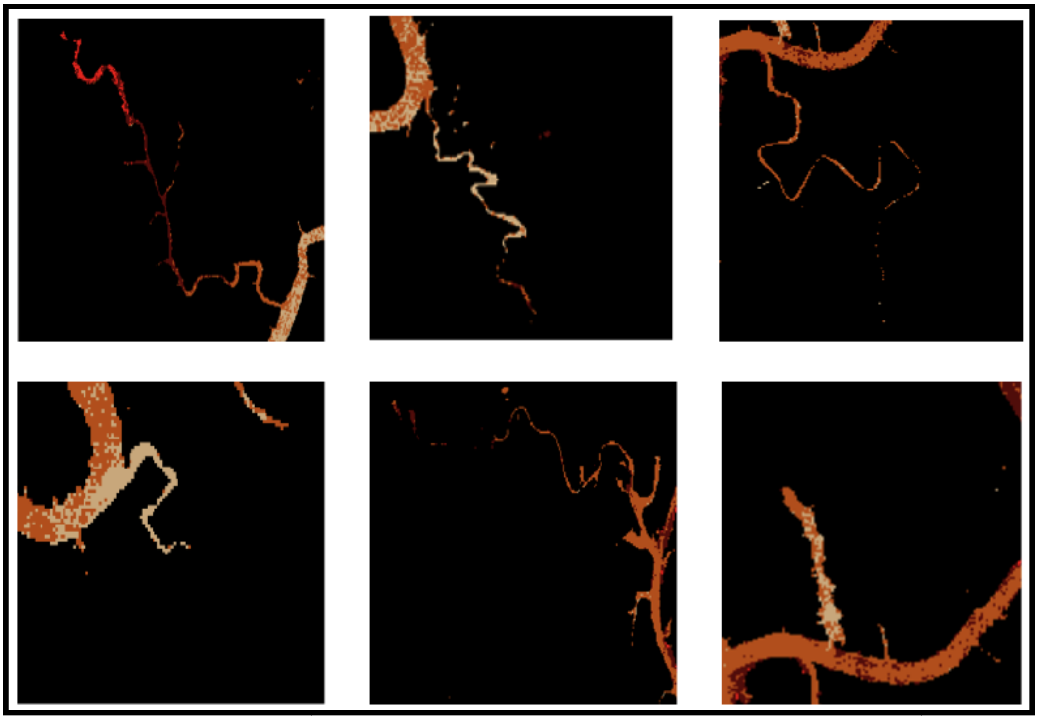

Fig. 10 Enlarged subsets of TSS concentrations in major tributaries inputting into Bankhead Lake. From top, left to bottom, right: Lower Big Yellow Creek, Shoal Creek, Valley Creek, Little Shoal Creek, Prescott Creek, and Lost Creek

*4.2.4 Estimating chlorophyll-*a *in Bankhead Reservoir during March conditions*

Chlorophyll-*a* is a significant contributor affecting lake trophic status. It is important in lake management to understand the spatial variability of chlorophyll in Bankhead Reservoir. Reflectance values were used in building both single band and band ratio regression models to estimate chlorophyll-*a* concentrations. The first type of models tested were linear equations using single band and logarithmically transformed reflectance as independent variables; chlorophyll-*a* and logarithmically transformed chlorophyll-*a* as dependent variables. Table 12 lists the R^2 and SEE for single band models and chlorophyll-*a*. TM band 4 was the most successful band for estimating chlorophyll-*a* concentration regardless of the model implemented. Hyperspectral investigations of algal-laden water have concluded chlorophyll-*a* has a peak reflectance at the boundary between the red (TM3) and NIR (TM4) wavelength regions which supports the significant relationship observed between TM band 4 reflectance and chlorophyll-*a* found in Bankhead Reservoir (Han 1997). Nas *et al.* (2010) found a significant relationship existed between TM 4 and chlorophyll-*a* concentrations in Lake Beysehir, Turkey.

Table 12 R^2 and **SEE (μgl^{-1})** for single band models

Chlorophyll-a Regression Models	TM 1	TM 2	TM 3	TM 4
chlor-a = $y_0 + a * b_j$	0.06**(1.07)**	0.19 **(0.99)**	0.01 **(1.09)**	0.64 **(0.66)**
chlor-a = $y_0 + a * \log(b_j)$	0.05 **(1.07)**	0.18 **(0.99)**	0.01 **(1.09)**	0.66 **(0.64)**
log(chlor-a) = $y_0 + a * b_j$	0.06 **(1.14)**	0.18 **(1.13)**	0.01 **(1.14)**	0.60 **(1.09)**
log(chlor-a) = $y_0 + a * \log(b_j)$	0.05 **(1.14)**	0.19 **(0.05)**	0.01 **(1.14)**	0.62 **(1.09)**

The second type of bivariate models were linear equations established using band ratio reflectance and logarithmically transformed band ratio reflectance as independent variables; chlorophyll-*a*, and logarithmically transformed chlorophyll-*a* as dependent variables. Kloiber *et al.* (2002) proved band ratios provide useful relationships with chlorophyll-*a*. Table 13 lists the R^2 and SEE for band ratio models and chlorophyll-*a* concentrations. R14 had the strongest relationship of all band ratios with chlorophyll-*a* concentration regardless of the model type. Nas *et al.* also found R4/1 had a significant relationship with chlorophyll-*a* and explained 39% of the variance observed. Chlorophyll has a strong absorption in band 1 and peak reflectance in the NIR bands and thus has a significant relationship with R1/4.

Table 13 R^2 and **SEE (μgl^{-1})** for band ratio models estimating chlorophyll-*a*

Chlorophyll-a Regression Models	R1/2	R1/3	R1/4	R2/3	R2/4	R3/4
chlor-a = $y_0 + a * (b_j/b_k)$	0.02 **(1.09)**	0.04 **(1.08)**	0.59 **(0.70)**	0.08 **(1.05)**	0.54 **(0.75)**	0.08 **(0.69)**
chlor-a = $y_0 + a * \log(b_j/b_k)$	0.02 **(1.08)**	0.04 **(1.08)**	0.56 **(0.72)**	0.08 **(1.05)**	0.51 **(0.77)**	0.08 **(0.68)**
chlor-a = $y_0 + a * (\log b_j/\log b_k)$	0.03 **(1.08)**	0.04 **(1.07)**	0.54 **(0.75)**	0.08 **(1.05)**	0.46 **(0.81)**	0.08 **(1.10)**
log(chlor-a) = $y_0 + a * (b_j/b_k)$	0.01 **(1.14)**	0.04 **(1.14)**	0.56 **(1.09)**	0.60 **(1.14)**	0.51 **(1.10)**	0.58 **(1.09)**
log(chlor-a) = $y_0 + a * \log(b_j/b_k)$	0.02 **(1.14)**	0.04 **(1.14)**	0.53 **(1.09)**	0.62 **(1.14)**	0.48 **(1.10)**	0.59 **(1.09)**
log(chlor-a) = $y_0 + a * (\log b_j/\log b_k)$	0.02 **(1.14)**	0.04 **(1.14)**	0.50 **(1.10)**	0.00 **(1.14)**	0.43 **(1.10)**	0.00 **(1.14)**

The band ratio regression model was chosen to estimate chlorophyll-*a* in Bankhead Reservoir and is considered superior to the others tested based on correlation coefficients, SEE, actual vs. predicted chlorophyll-*a* concentrations and visual interpretation of the maps produced. The band ratio linear regression model employed to map chlorophyll-*a* in Bankhead Reservoir during observed spring water quality conditions had the form of:

$$\log(\text{chlor-}a) = y_0 + a * \log(b_j/b_k) \qquad (3)$$

Where chlor-*a* is chlorophyll-a concentration ($\mu g l^{-1}$);y_0 is the regression constant; a is the regression coefficient; and b_j/b_k is TM R1/4.

Figure 11 summarizes the statistical results using the regression model described in equation (3) used to estimate chlorophyll-*a* concentrations. The R^2 value was 0.53 ($p<0.007$) and the SEE was 0.039 (1.094 $\mu g 1^{-1}$). Higher concentrations of chlorophyll-*a* increase the reflectance in TM 4 faster than in the shorter wavelength TM 1. Figure 12 shows the comparison of the estimated TSS with the actual *in situ* sample data. The R1/4 band ratio model using equation (3) provides reasonable TM derived chlorophyll-*a* values and were on average slightly higher than the *in situ* data. Using this model in the ERDAS imagine software, a chlorophyll-*a* concentration map was produced (Figure 13). The map successfully characterizes the spatial pattern of chlorophyll-*a* in Bankhead Reservoir of the Black Warrior River during observed spring conditions.

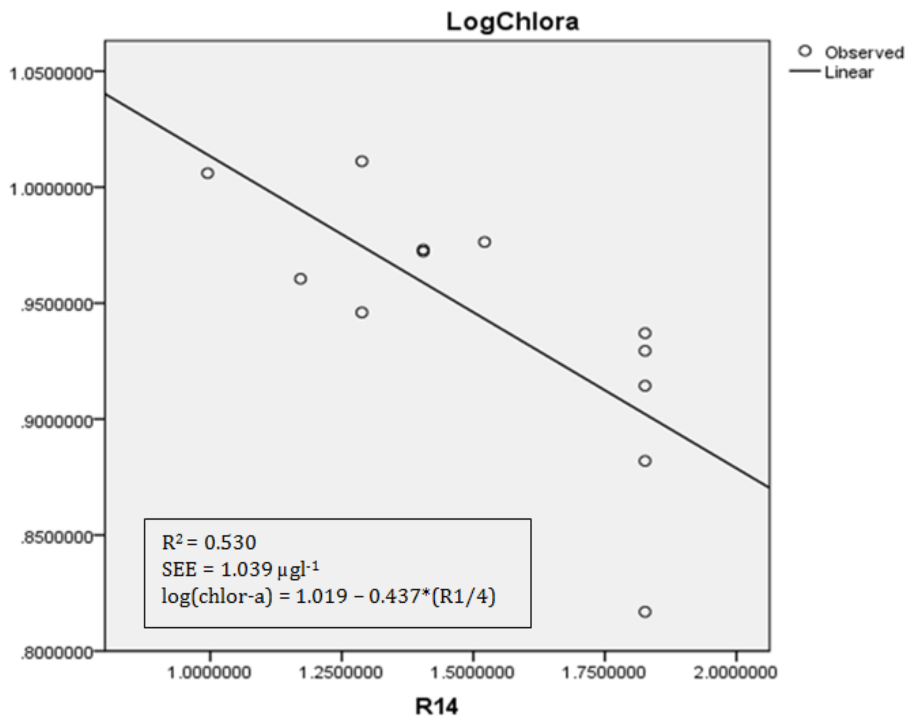

Fig. 11 Statistical results using chosen regression model to estimate March chlorophyll concentrations

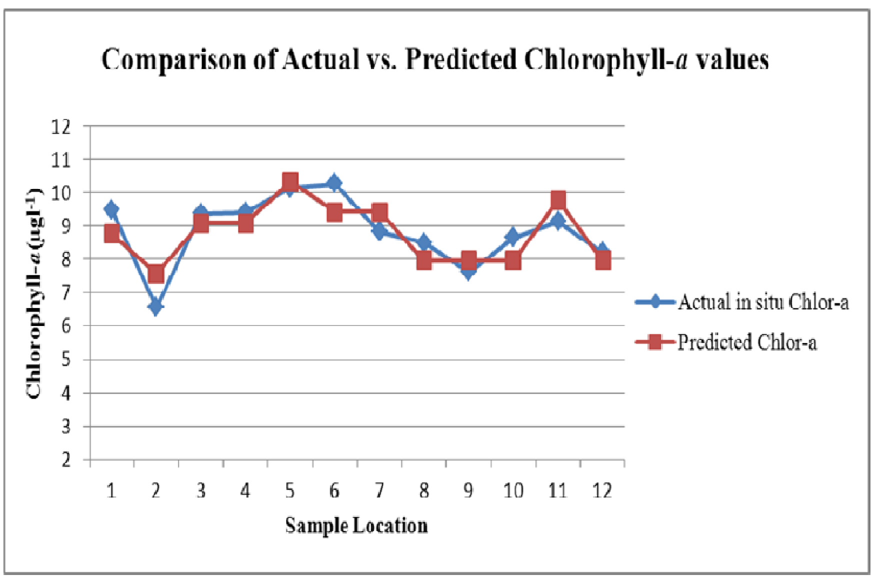

Fig. 12 Comparison of Actual vs. Predicted March TSS concentrations

During March conditions chlorophyll-*a* in Bankhead Reservoir ranged from 4.05 to 12.5 $\mu g l^{-1}$. The map indicates that chlorophyll-*a* is greater in the lower portions of Bankhead Reservoir's main stem and decreases as you move upstream to the mid-reservoir. The higher concentrations observed in the lower reservoir could be resulting from slower flow near the dam forebay making it more conducive for algae growth. Elevated levels also occurred in the main stem where the Locust Fork inputs into the lake. The upper reaches of the Locust Fork generally had chlorophyll-*a* concentrations between 9.12 – 12.5 $\mu g l^{-1}$. Bankhead Reservoir's Mulberry Fork had concentrations ranging from 4.05 to 11.12 $\mu g l^{-1}$. The upper Mulberry Fork inputting into the lake had higher chlorophyll concentrations (9.12 – 11.12 $\mu g l^{-1}$). The low chlorophyll levels were expected for this time of year.

Several tributary embayments were also mapped for chlorophyll-*a*. Figure 14 displays the enlarged subsets of chlorophyll concentrations in major tributaries inputting into Bankhead Lake. Shoal Creek, Little Shoal Creek, and Valley Creek have the highest concentrations of all tributaries contributing to Bankhead Reservoir (9.12 – 12.5 $\mu g l^{-1}$). Big Yellow Creek embayment had lower chlorophyll-*a* concentrations than any other tributary inputting into the reservoir (4.05 – 11.18 $\mu g l^{-1}$) and levels increased downstream toward the reservoir. Lost Creek inputs into the Mulberry Fork of Bankhead Reservoir and the lower embayment had chlorophyll concentrations ranging from 4.05 to 6.71 $\mu g l^{-1}$ while its upper embayment contained higher levels (9.12 – 12.5 $\mu g l^{-1}$). While the observed chlorophyll concentrations are acceptable for this time of year and pose no threat to the river it is important to understand the spatial variation found in Bankhead Reservoir during late winter/early spring background conditions for comparison in future synoptic studies of the reservoir.

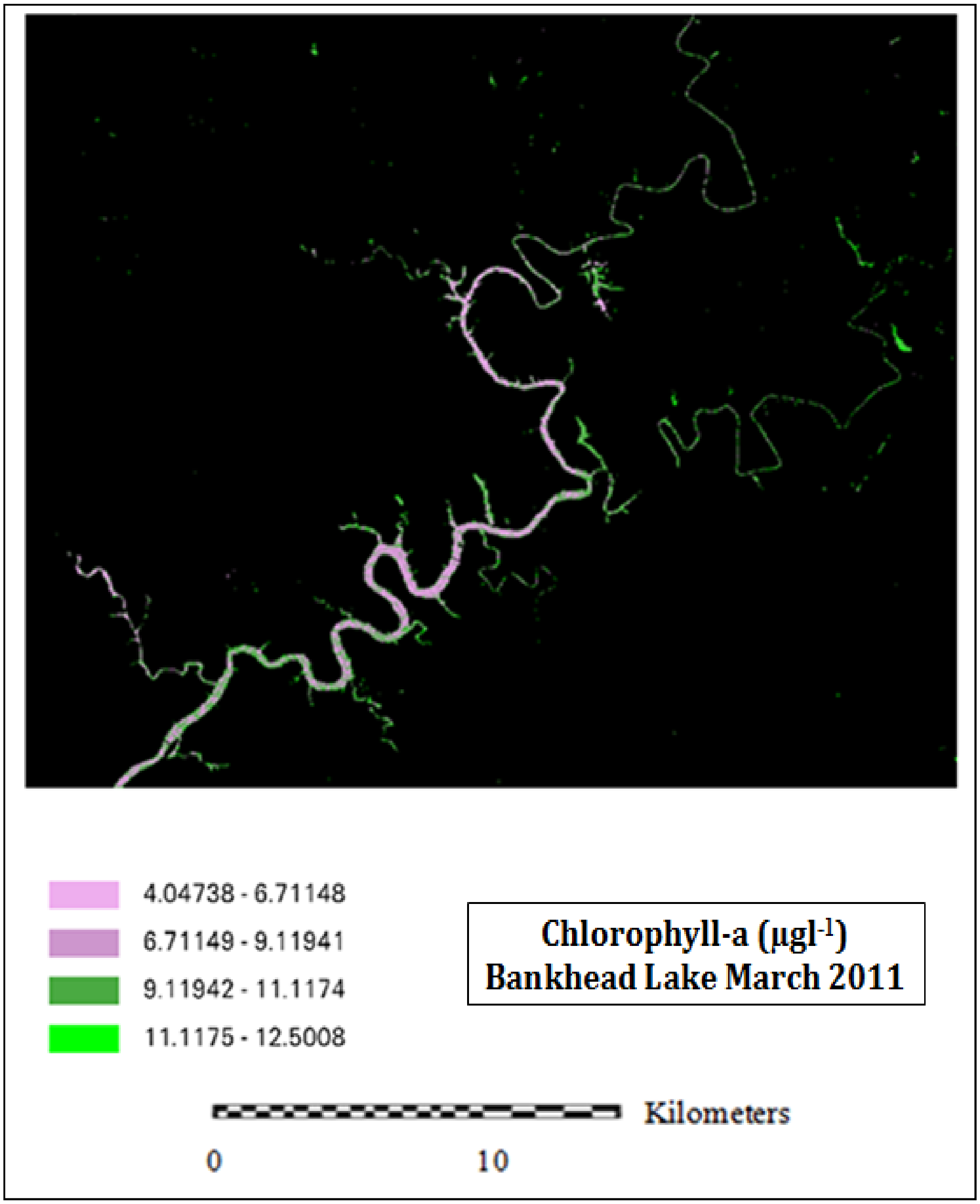

Fig. 13 Chlorophyll-*a* concentration map of Bankhead Reservoir during observed March conditions

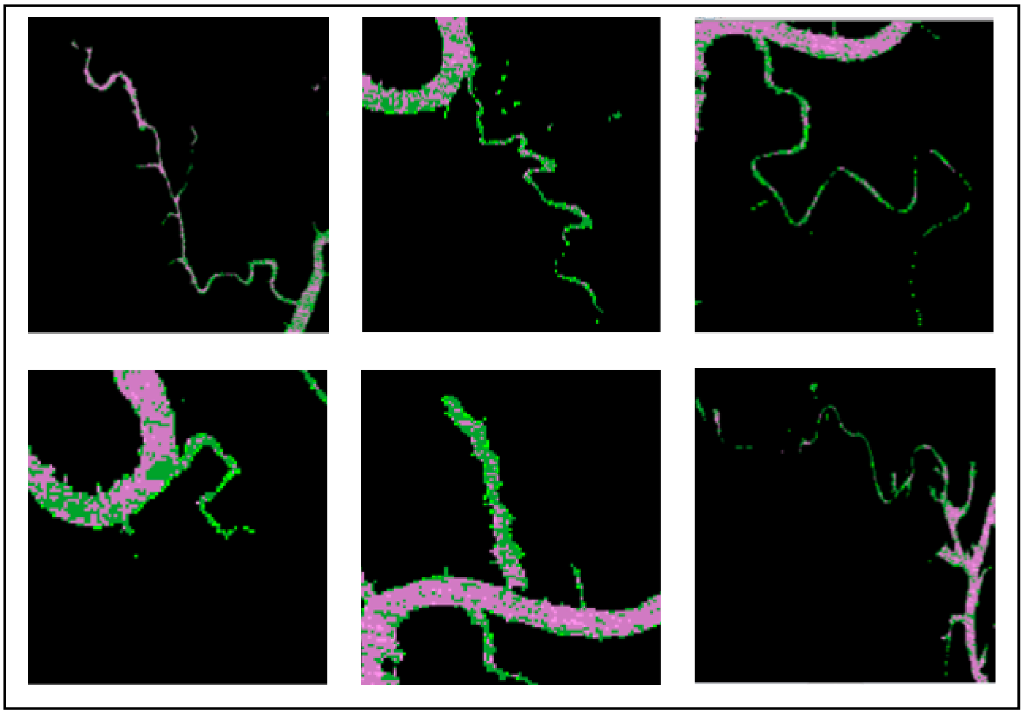

Fig. 14 Enlarged subsets of chlorophyll concentrations in major tributaries inputting into Bankhead Lake. From top, left to bottom, right: Lower Big Yellow Creek, Shoal Creek, Valley Creek, Little Shoal Creek, Prescott Creek, Lost Creek

4.3 August data

4.3.1 In-situ water quality data

Table 14 August TSS, chlorophyll-a and SDD in Bankhead Reservoir

Sample	TSS (μgl^{-1})	Chlorophyll-*a* (μgl^{-1})	SDD (meters)
1	1258.81	21.20	1.10
2	926.68	22.63	1.25
3	938.63	15.80	1.10
4	926.47	13.89	1.15
5	962.13	17.73	1.40
6	956.93	22.06	1.40
7	971.53	15.65	1.35
8	962.17	22.26	1.20
9	931.49	20.30	1.30
10	934.32	21.99	1.35
11	938.33	21.28	1.10
12	965.75	26.12	1.10

Table 14 shows the laboratory-measured total suspended solids and chlorophyll-*a* for the twelve sampling sites found in August. The mean TSS was 972.77 μgl^{-1} and had a standard deviation of 91.53 μgl^{-1} (table 15). The highest amount of TSS was recorded at site one towards the upper end of the mid-reservoir. TSS concentrations were significantly higher than during March conditions. TSS was expected to be lower due to discharge during low-flow conditions (84 ft^3s^{-1}) and increased vegetation helping to decrease erosion. The elevated TSS concentrations may in part be a reflection of the increased organic algal biomass in the reservoir during this time of year. The low-flow associated with the higher TSS values could indicate the increase is a result of increased point source discharges. The highest amount of TSS was recorded at site one towards the upper end of the mid-reservoir. The mean chlorophyll-*a* concentration was much

Table 15 Descriptive statistics for August water quality data

Parameter	N	Minimum	Maximum	Mean	Std.
Total Suspended Solids (µg/l)	12	926.47	1258.81	972.77	91.53
Chlorophyll-a (µg/l)	12	13.89	26.12	20.08	3.57

higher (20.08 μgl^{-1}) than in March and had a standard deviation of 3.57 μgl^{-1}. The highest amounts of chlorophyll-*a* were found at sites two and six and the lowest concentration was found at site four. Elevated chlorophyll-*a* was expected in Bankhead Reservoir during this time of year as a result of excess vegetation and lower flow conditions.

4.3.2 Correlating water quality and reflectance

Statistical techniques were used to derive correlations between TM bands 1-4 spectral data and TSS and chlorophyll-*a*. Table 16 shows the pixel reflectance for each sampling location extracted from the August Landsat TM image. Table 17 lists the Pearson's correlation coefficients between both August TSS and chlorophyll-*a* concentrations and TM bands and band ratios utilized in this study. The strengths of correlation between bands and band ratios differ for each water quality parameter.

Table 16 TM bands 1-4 reflectance for each sampling site

Sample	TM Band 1	TM Band 2	TM Band 3	TM Band 4
1	0.021	0.021	0.019	0.017
2	0.023	0.024	0.021	0.020
3	0.021	0.024	0.017	0.020
4	0.021	0.021	0.017	0.013
5	0.019	0.018	0.017	0.013
6	0.019	0.021	0.017	0.020
7	0.021	0.021	0.017	0.013
8	0.019	0.021	0.019	0.017
9	0.018	0.018	0.017	0.017
10	0.018	0.018	0.014	0.017
11	0.018	0.018	0.014	0.020
12	0.018	0.021	0.019	0.017

No single band or band ratio had a correlation with TSS during August water quality conditions. Band 3 displayed the strongest single band correlation to TSS ($r = 0.286$); Band ratio R2/3 was found to have the overall strongest relationship ($r = -0.293$) to TSS found in Bankhead Reservoir during August. However, neither relationship was significant. The August Landsat image used in this study was impacted by cloud cover which may have had some impact on the weak relationship found between TSS and single bands and band ratios. Chlorophyll-*a* was significantly and most highly correlated with band ratios R1/3, R1/4, R2/3, and R2/4. Algal-laden waters have a distinct spectral curve with absorption in the blue region, a maximum reflectance in the green region, absorption in the red region, and a reflectance peak at the red/NIR spectral boundary (Han 1997). All band ratios have a negative correlation due to the reflectance peak at the band 3/band 4 spectral boundary which is in the denominator of the band ratios correlated with chlorophyll.

Table 17 Pearson correlation coefficients between water quality parameters and various Landsat TM band and band ratios.

August Data		TM 1	TM 2	TM 3	TM 4	R1/2	R1/3	R1/4	R2/3	R2/4	R3/4
Total Suspended Solids	r	0.15	0.06	0.29	-0.09	0.09	-0.23	0.11	-0.29	0.09	0.22
	Sig. *	0.63	0.85	0.37	0.78	0.77	0.47	0.73	0.36	0.78	0.49
Chlorophyll-*a*	r	-0.32	-0.10	0.33	**0.46**	-0.32	**-0.69**	**-0.64**	**-0.51**	**-0.60**	-0.28
	Sig.*	0.30	0.77	0.29	**0.13**	0.31	**0.01**	**0.02**	**0.09**	**0.04**	0.37

4.3.3 Estimating TSS in Bankhead Reservoir during August conditions

Reflectance values were used in an attempt to build both single band and band ratio regression models for TSS estimation. The first bivariate regression models were linear and tested single band reflectance and logarithmically transformed reflectance as independent variables and TSS and logarithmically transformed TSS as dependent variables. However, using a 2nd order quadratic polynomial equation instead of a linear equation provided higher correlation coefficients and was implemented for the August TSS data. Table 18 lists the R^2 and standard

Table 18 R^2 and **SEE (μgl-^{1})** for single band models estimating TSS

TSS Regression Models	TM 1	TM 2	TM 3	TM 4
$tss = y_0 + a * b_j - b * (b_j)^2$	0.14 **(93.88)**	0.15 **(93.11)**	0.13 **(94.50)**	0.14 **(94.07)**
$tss = y_0 + a * \log(b_j) - b * \log(b_j)^2$	0.13 **(94.26)**	0.15 **(93.11)**	0.11 **(94.57)**	0.14 **(94.07)**
$\log(tss) = y_0 + a * b_j - b * (b_j)^2$	0.14 **(1.09)**	0.16 **(1.09)**	0.13 **(1.09)**	0.14 **(1.09)**
$\log(tss) = y_0 + a * \log(b_j) - b * \log(bj)^2$	0.14 **(1.09)**	0.16 **(1.09)**	0.11 **(1.09)**	0.14 **(1.09)**

error of estimate (SEE) for single band models and TSS concentrations. No single band had a significant relationship to August TSS concentrations.

The band ratio regression models were established using band ratio reflectance and logarithmically transformed ratio reflectance as independent variables and TSS and logarithmically transformed TSS as dependent variables. Table 19 lists the R^2 and SEE for band ratio models and TSS concentrations. No band ratio had a significant relationship with TSS and thus an accurate water quality map for TSS conditions during August was unable to be produced. The weak relationship between TSS and reflectance may have been impacted by haze from the clouds in the atmosphere on the day of image acquisition. Bankhead Reservoir is a constantly moving riverine system, which could also contribute to the weak relationship exhibited between TSS and reflectance.

Table 19 R^2 and **SEE (μgl^{-1})** for band ratio models estimating TSS

TSS Regression Models	R1/2	R1/3	R1/4	R2/3	R2/4	R3/4
$tss = y_0 + a * (b_j/b_k) - b * (b_j/b_k)^2$	0.02 **(100.33)**	0.13 **(94.19)**	0.16 **(92.92)**	0.09 **(91.78)**	0.09 **(96.39)**	0.05 **(93.57)**
$tss = y_0 + a * \log(b_j/b_k) - b * \log(b_j/b_k)^2$	0.02 **(100.37)**	0.14 **(94.11)**	0.12 **(92.92)**	0.09 **(91.68)**	0.07 **(97.37)**	0.05 **(93.36)**
$tss = y_0 + a * (\log b_j/\log b_k) - b * (\log b_j/\log b_k)^2$	0.01 **(95.52)**	0.14 **(94.1)**	0.11 **(95.75)**	0.08 **(91.87)**	0.07 **(97.81)**	0.06 **(93.20)**
$\log(tss) = y_0 + a * (b_j/b_k) - b * (b_j/b_k)^2$	0.01 **(8.69)**	0.13 **(3.35)**	0.16 **(2.92)**	0.09 **(1.09)**	0.10 **(4.34)**	0.05 **(1.09)**
$\log(tss) = y_0 + a * \log(b_j/b_k) - b * \log(b_j/b_k)^2$	0.01 **(1.10)**	0.13 **(1.09)**	0.12 **(1.09)**	0.09 **(1.09)**	0.08 **(1.09)**	0.06 **(1.09)**
$\log(tss) = y_0 + a * (\log b_j/\log b_k) - b * (\log b_j/\log b_k)^2$	0.01 **(1.09)**	0.13 **(1.09)**	0.10 **(1.09)**	0.09 **(1.09)**	0.07 **(1.09)**	0.06 **(1.09)**

*4.3.4 Estimating chlorophyll-*a *in Bankhead Reservoir during August conditions*

Understanding the spatial variation of chlorophyll-*a* during the growing season when concentrations are elevated is of extreme importance in lake management. Observing Landsat imagery from late summer allows for a direct estimate of trophic conditions at their maximum (Kloiber *et al.* 2002). Reflectance values were used in building both single band and band ratio regression models to estimate chlorophyll-*a* concentrations. The first type of bivariate models tested were linear equations and used single band reflectance and logarithmically-transformed reflectance as independent variables; chlorophyll-*a* and logarithmically-transformed chlorophyll-*a* as dependent variables. However, using a 2nd order quadratic polynomial instead of a linear regression equation provided much higher correlation coefficients (r) and was thus chosen for the August data. Table 20 lists the R^2 and SEE for single band models and chlorophyll-*a*. TM band 4 was the most successful band for estimating chlorophyll-*a* concentration regardless of the form of regression model implemented. Hyperspectral investigations of algal-laden water have concluded chlorophyll-*a* has a peak reflectance at the boundary between the red and NIR wavelength regions which supports the significant relationship observed between TM band 4 reflectance and chlorophyll-*a* found in Bankhead Reservoir during both March and August conditions (Han 1997). TM 4 has been found to have a significant relationship with chlorophyll-*a* concentrations (Nas *et al*. 2010).

Table 20 R^2 and **SEE ($\mu g l^{-1}$)** for single band models estimating chlorophyll-*a*

Chlorophyll-a Regression Models	TM 1	TM 2	TM 3	TM 4
chlor-a = $y_0 + a * b_j - b * (b_j)^2$	0.46 **(2.91)**	0.01 **(3.92)**	0.26 **(3.39)**	0.59 **(2.52)**
chlor-a = $y_0 + a * \log(b_j) - b * \log(b_j)^2$	0.44 **(2.95)**	0.01 **(3.92)**	0.30 **(3.29)**	0.59 **(2.52)**
log(chlor-a) = $y_0 + a * b_j - b * (b_j)^2$	0.46 **(1.16)**	0.02 **(1.23)**	0.26 **(1.19)**	0.61 **(1.14)**
log(chlor-a) = $y_0 + a * \log(b_j) - b * \log(b_j)^2$	0.44 **(1.17)**	0.02 **(1.23)**	0.30 **(1.19)**	0.61 **(1.14)**

The second type of bivariate models were quadratic equations established using band ratio reflectance and logarithmically transformed ratio reflectance as independent variables; chlorophyll-*a*, and logarithmically transformed chlorophyll-*a* as dependent variables. Table 21 lists the R^2 and SEE for band ratio models and chlorophyll-*a* concentrations. Chlorophyll- *a* had the highest R^2 and lowest SEE with band ratio R1/4 regardless of the model type. R4/1 has been found to have a significant relationship with chlorophyll-*a* concentrations (Nas *et al.* 2010). Chlorophyll has a strong absorption in band 1 and a peak reflectance in the NIR bands which supports the significant relationship observed between R1/4 and chlorophyll-*a* found in Bankhead Reservoir during both March and August conditions.

Table 21 R^2 and **SEE (μgl^{-1})** for band ratio models estimating chlorophyll-*a*

Chlorophyll-a Regression Models	R1/2	R1/3	R1/4	R2/3	R2/4	R3/4
$chlor\text{-}a = y_0 + a * (b_j/b_k) - b * (b_j/b_k)^2$	0.10 **(3.73)**	0.49 **(2.81)**	0.58 **(2.57)**	0.26 **(3.23)**	0.50 **(2.78)**	0.08 **(3.59)**
$chlor\text{-}a = y_0 + a * \log(b_j/b_k) - b * \log(b_j/b_k)^2$	0.10 **(3.73)**	0.49 **(2.81)**	0.56 **(2.62)**	0.25 **(3.24)**	0.49 **(2.82)**	0.06 **(3.62)**
$chlor\text{-}a = y_0 + a * (\log b_j/\log b_k) - b * (\log b_j/\log b_k)^2$	0.09 **(3.56)**	0.51 **(2.76)**	0.55 **(2.64)**	0.26 **(3.22)**	0.48 **(2.85)**	0.05 **(3.64)**
$\log(chlor\text{-}a) = y_0 + a * (b_j/b_k) - b * (b_j/b_k)^2$	0.08 **(1.22)**	0.45 **(1.16)**	0.61 **(1.14)**	0.26 **(1.18)**	0.55 **(1.15)**	0.10 **(1.21)**
$\log(chlor\text{-}a) = y_0 + a * \log(b_j/b_k) - b * \log(b_j/b_k)^2$	0.08 **(1.22)**	0.45 **(1.16)**	0.59 **(1.14)**	0.26 **(1.18)**	0.57 **(1.15)**	0.08 **(1.21)**
$\log(chlor\text{-}a) = y_0 + a * (\log b_j/\log b_k) - b * (\log b_j/\log b_k)^2$	0.07 **(1.21)**	0.48 **(1.16)**	0.58 **(1.14)**	0.27 **(1.18)**	0.53 **(1.15)**	0.07 **(1.21)**

The band ratio regression model was chosen to estimate chlorophyll-*a* in Bankhead Reservoir. The regression model implemented is considered superior to the others tested based on correlation coefficients, SEE, actual vs. predicted chlorophyll-*a* concentrations and visual interpretation of the maps produced. The August Landsat image was impacted by haze created from patches of clouds. Equations using band ratios may potentially offer an advantage when atmospheric interference is high. The band ratio linear regression model employed to map chlorophyll-a in Bankhead Reservoir during observed August water quality conditions had the form of:

$$\log(chlor\text{-}a) = y_0 + a * (b_j/b_k) - b *(b_j/b_k)^2 \quad (4)$$

Where chlor-*a* is chlorophyll-a concentration (μgl^{-1});y_0 is the regression constant; a,b are the regression coefficients; and bj/bk is TM R1/4.

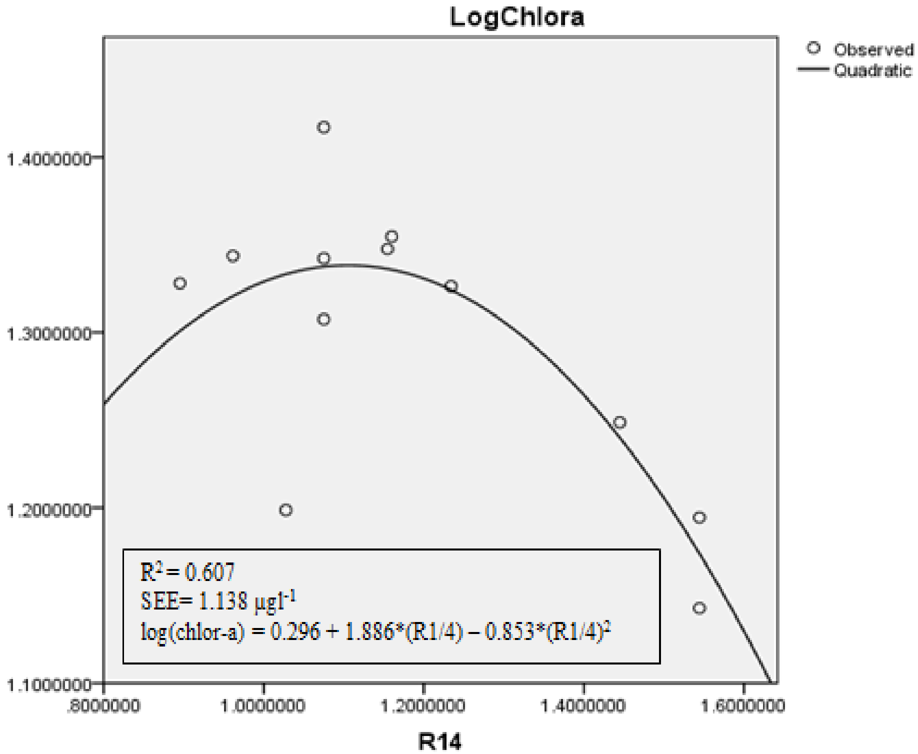

Fig.15 Statistical results using chosen regression model to estimate August chlorophyll concentrations

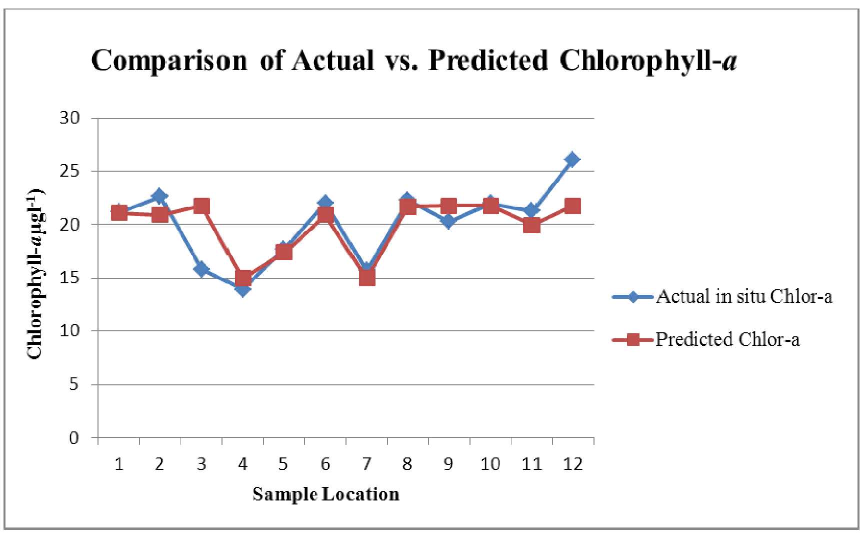

Fig. 16 Comparison of Actual vs. Predicted March TSS concentrations

Figure 15 summarizes the statistical results using the regression model described in equation (4) and R1/4 as the independent variable to estimate chlorophyll-*a* concentrations. The R^2 value was 0.607 ($p<0.015$) and the SEE was 0.056 (1.138 $\mu g l^{-1}$). Higher concentrations of chlorophyll-*a* increase the reflectance in TM 4 faster than in the shorter wavelength TM 1. Figure 16 shows the comparison of the estimated chlorophyll-*a* with the actual *in situ* chlorophyll-*a* data. The R1/4 model using equation (4) provides reasonable TM derived chlorophyll-*a* values and were on average slightly lower than *in situ* data indicating the map produced is a slight underestimation of actual chlorophyll conditions found in the lake.

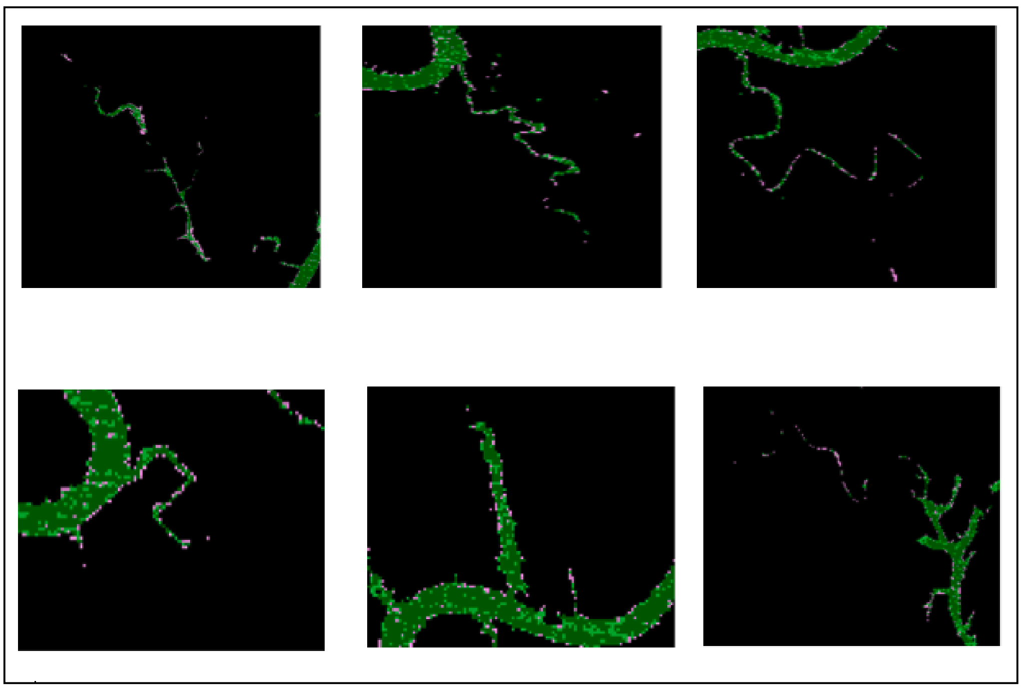

Fig. 17 Enlarged subsets of chlorophyll concentrations in major tributaries inputting into Bankhead Lake. From top, left to bottom, right: Lower Big Yellow Creek, Shoal Creek, Valley Creek, Little Shoal Creek, Prescott Creek, Lost Creek

Using this model in the ERDAS imagine software, a chlorophyll-*a* concentration map was produced (Figure 18). The spatial distribtion of chlorophyll-*a* found in Bankhead Reservoir during late summer conditions was mapped excluding the areas of the lake impacted by cloud cover. The water quality map of Bankhead Reservoir during August was impacted by cloud cover causing small portions of the Lake and its tributaries to be omitted. The map successfully characterizes the spatial pattern of chlorophyll-*a* in Bankhead Reservoir of the Black Warrior River during observed August conditions and indicates the mainstem and tributary embayments of Bankhead Reservoir have eutrophic levels exceeding 16 μgl^{-1}. Figure 17 displays enlarged subsets of chlorophyll concentrations in major tribuatries inputting into Bankhead Reservoir. The majority of Bankhead's main stem and tributaries had eutrophic levels between 19.93 and 21.72 μgl^{-1}. Big Yellow Creek had the lowest concentrations found during August conditions ranging from 8.52 to 19.93 μgl^{-1}. The far upper reaches of the Locust Fork also contained lower chlorophyll concentrations (8.52 – 16.95 μgl^{-1}). Lost Creek displayed lower levels (8.52 – 16.95 μgl^{-1}) upstream from Bankhead Reservoir. However, the majority of Bankhead Reservoir and its tributaries exceed the maximum allowable level of 16 μgl^{-1}. According to Raschke (1993), a mean growing season limit of 15 μgl^{-1} of chlorophyll should be maintained for water supply reservoirs to limit filter clogging and taste/odor problems and also recommends below 25 μgl^{-1} of chlorphyll-*a* to maintain recreational aesthetic value. Further study is needed to understand the threat of growing season chlorophyll-*a* concentrations in Bankhead Reservoir.

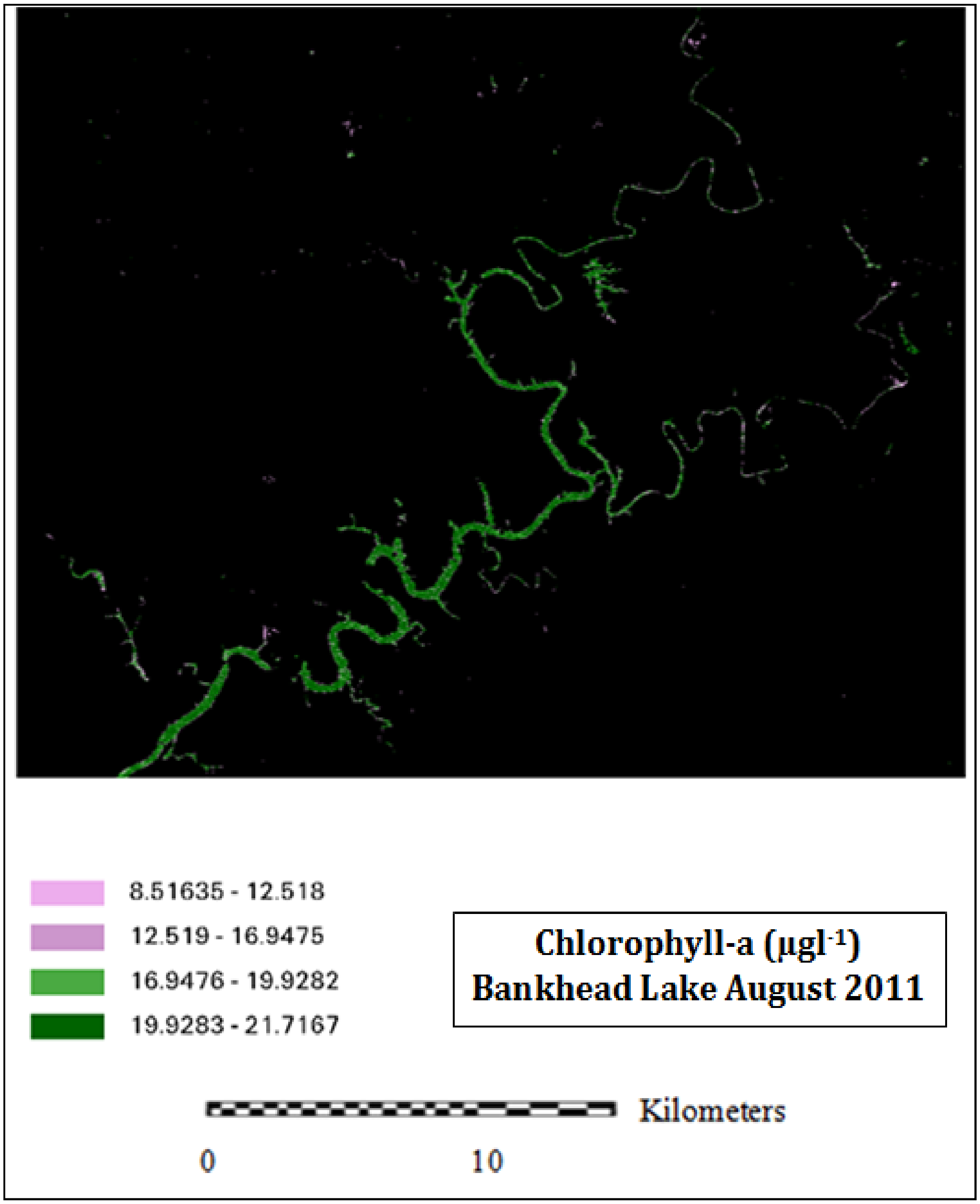

Fig. 18 Chlorophyll-*a* concentration map of Bankhead Reservoir during observed August conditions

5. Conclusions

The TSS concentrations found in Bankhead Reservoir were successfully mapped during March conditions. I found the linear regression model in the form of equation (2) to produce the map that most accurately estimates and displays TSS found within Bankhead Reservoir during observed March conditions. Single band TM 3 was found to be the most successful predictor of TSS, which supports several previous investigations using Landsat TM imagery to map suspended solids in inland water bodies. These findings suggest that the Landsat TM sensor successfully detected the variance. The highest TSS concentrations were found in the Mulberry and Locust Forks and gradually decreased towards the lower reservoir. The Big Yellow Creek and Lost Creek embayments contained the highest tributary TSS levels. Little Shoal Creek and Shoal Creek had slightly elevated TSS concentrations in their upper embayments near Shoal Creek Mine. Elevated TSS levels could be due to excess discharges from Shoal Creek Mine resulting from the recent precipitation event. For suspended solids management it is important to understand and maintain background levels within a water body to effectively protect aquatic life and while these TSS levels are still extremely low for this time of year and pose no threat to the river it is important to understand the spatial variation of TSS found in Bankhead Reservoir during late winter/early spring background conditions for comparison in future synoptic studies. An August TSS map was unable to be produced due to the weak relationship it exhibited with reflectance values. This was most likely a result of haze in the atmosphere at the time of image acquisition as well as the dynamic properties of the Black Warrior River. Further study is needed to understand the temporal distribution of TSS in Bankhead Reservoir.

Chlorophyll-*a* concentrations found in Bankhead Reservoir for both March and August conditions were successfully estimated. I found that both TM band 4 and R1/4 are significant predictors of chlorophyll-*a* concentrations during both late winter/early spring and late summer/early fall conditions. The linear regression model used for March was in the form of equation (3) and implemented log (R1/4) as the independent variable. A quadratic polynomial equation in the form of equation (4) using log (R1/4) as the independent variable most accurately estimated chlorophyll levels during August conditions. During March conditions chlorophyll-*a* was greater in the lower portions of Bankhead Reservoir’s main stem and could be a result of slower flow near the dam forebay making it more conducive for algae growth. Shoal Creek, Little Shoal Creek, and Valley Creek contained the highest chlorophyll concentrations of all tributaries contributing to Bankhead Reservoir in March. The August chlorophyll map is especially significant for management purposes as it shows the entire main stem of Bankhead Reservoir has chlorophyll-*a* concentrations exceeding 16 $\mu g l^{-1}$ during August conditions. Further study is needed to understand the threat these high chlorophyll-*a* levels pose on the lake.

My study successfully demonstrates that remote sensing coupled with a small number of field samples can provide an accurate and synoptic view of Bankhead Reservoir’s background water quality conditions during both March and August conditions. Only a limited number of intensive studies have been conducted on Bankhead Reservoir due to the cost and resources necessary to sample areas distributed throughout the entire system. I have added valuable information on the regression models and independent variables most successfully estimating water quality concentrations for both March and August conditions found within Bankhead Reservoir of the Black Warrior River. The results from this study serve as baseline water quality maps providing a complete spatial view of TSS and chlorophyll-*a* concentrations and capable of identifying water quality problems critical for effective surface water management. The spatial variations in Bankhead Reservoir’s water quality can be used as background levels for comparison in the future management of the watershed. This study successfully demonstrates remote sensing can be effectively used for synoptic water quality monitoring in reservoirs.

6. References

ADEM. (2011a). *ADEM Administrative Code 335-6-10*, *Water Quality Criteria*. Water Quality Division, Alabama Department of Environmental Management. Montgomery, AL. Retrieved 27 September 2011

ADEM. (2011b). *ADEM Administrative Code 335-6-11*, *Water use classifications for Interstate and Intrastate Waters*. Water Quality Division, Alabama Department of Environmental Management. Montgomery, AL. Retrieved 27 September 2011

ADEM. (2010). *Alabama's 2010 Integrated Water Quality Monitoring and Assessment Report*. Alabama Department of Environmental Management. Montgomery, AL.

ADEM. (2004a). Black Warrior River Watershed Management Plan. Alabama Department of Environmental Management. Montgomery, AL. Retrieved 15 February 2011 from: http://adem.alabama.gov/programs/water/nps/files/BlackWarriorBMP.pdf.

ADEM. (2004b). *Intensive Water Quality Survey of Warrior River Basin Reservoirs: 2002*. Field Operations Division, Alabama Department of Environmental Management. Montgomery, AL. Retrieved 01 October 2010 from: http://www.adem.state.al.us/ programs/water/wqsurvey/cnt.

ADEM. (2004c). Surface Water Quality Screening Assessment of the Cahaba and Black Warrior River Basins-2002. Aquatic Assessment Unit, Field Operations Division, Alabama Department of Environmental Management. Montgomery, AL.

ADEM. (2009a). National Pollutant Discharge Elimination System Individual Permit, Drummond Company, Inc., Shoal Creek Mine, AL0062421. Alabama Department of Environmental Management. Montgomery, AL.

ADEM. (2009b). *Nutrient Criteria Implementation Plan, State of Alabama*. Alabama Department of Environmental Management. Montgomery, AL. Retrieved 05 March 2011 from: http://adem.alabama.gov/programs/water/.../2010AL-IWQMAR.pdf

ADEM. (2005). *Surface Water Quality Monitoring Strategy*. Water Quality Division, Alabama Department of Environmental Management. Montgomery, AL. Retrieved 05 November 2010 from: http://www.adem.state.al.us/programs/water/waterquality/cnt.

AFA. (1996). *Eutrophication of Alabama Lakes*. Position paper. Alabama Fisheries Association. Montgomery, Alabama.

AFC. (2010). Forests at the Crossroads: Alabama's Forest Assessment and Resource Strategy. Alabama Forestry Commission. State of Alabama. Retrieved 05 November 2011 from: http://media.al.com/bn/other/ALABAMA_ASSESSMENT_FINAL.pdf

American Rivers. (2011). *America's Most Endangered Rivers.* American Rivers. Washington, D.C.

APHA. (1989). Standard Methods for the Examination of Water and Wastewater. 17th ed. American Public Health Association. Washington, DC.

APHA. (1992). Standard Methods for the Examination of Water and Wastewater. 18th ed. American Public Health Association. Washington, DC.

Arar, E. J., Collins, G.B. (1997). *Method 445.0 In vitro determination of chlorophyll-a and pheophytin-a in marine and freshwater algae by fluorescence, revision 1.2*. National Exposure Research Laboratory, Office of Research and Development, U.S. Environmental Protection Agency. Cincinnati, Ohio.

Bayne, D.R., Maceina, M.J., Reeves, N.C. (1994). Zooplankton, fish and sports fishing quality among four Alabama and Georgia reservoirs of varying trophic status. *Lake and Reservoir Management* 8 (2): 153-163.

Clean Water Act. (1972). 33 U.S.C. § 1251 et seq. 2002. Retrieved from http://esp.senate.gov/water/pdf.

Berry, W., Rubenstein, N., Melzian, B., Hill, B. (2003). *The Biological Effects of Suspended and Bedded Sediment (SABS) in Aquatic systems: A Review*. An Internal EPA report. Office of Research and Development, Environmental Protection Agency. Retrieved 10 March 2011 from: http://www.epa.gove/waterscience/criteria/sediment/pdf/ appendix1.pdf.

Brivio, P.A., Giardino, C., Zilioli, E. (2001). Determination of chlorophyll concentration changes in Lake Gard using an image-based radiative transfer code for Landsat TM images, *International Journal of Remote Sensing* 22:487-502.

Chavez, P.S. Jr. (1988). An improved dark-object subtraction technique for atmospheric scattering correction of multi-spectral data. *Remote Sensing of Environment* 24:459-479.

Chavez, P.S. Jr. (1996). Image-based atmospheric corrections- revisited and improved. *Photogrammetric Engineering and Remote Sensing* 62:1025-1036.

Congalton, R.G. (1991). A Review of assessing the accuracy of classifications of remotely sensed data. *Remote Sensing of the Environment* 37:35-46

Dekker, A.G., Vos, R.J., Peters, S.W.M. (2002). Analytical algorithms for lake water TSM estimation for retrospective analysis of TM and SPOT sensor data. *International Journal of Remote Sensing* 23: 15-35.

Dekker, A.G., Malthus, T.J., Seyhan, E. (1991). Quantitative modeling of inland water quality for high-resolution MSS systems. *Geoscience and Remote Sensing* 29:89-95.

Dekker, A.G., Peters, S.W.M. (1993). The use of the Thematic Mapper for the analysis of eutrophic lakes: A case study in the Netherlands. *International Journal of Remote Sensing* 14 (5): 799-822.

Dwivedi, R.M., Narain, A. (1987). Remote sensing of phytoplankton an attempt from the Landsat Thematic Mapper. *International Journal of Remote Sensing* 8:1563-1569.

EIA. (2005). Annual Coal Report 2004. Energy Information Administration. Office of Coal, Nuclear, Electric, and Alternative Fuels, US Department of Energy. Washington DC.

Ekstrand, S. (1992). Landsat TM based quantification of chlorophyll-a during algal blooms in coastal waters. *International Journal of Remote Sensing* 3:1913-1926.

Ekstrand, S. (1998). Determination of algal production in an industrial wastewater plume using Landsat TM imagery. *IVL (Swedish Environmental Research Institute) report B-1304*. Stockholm, Sweden. Retrieve 10 August 2011 from: http://www.ivl.se/download/18.7df4c4e812d2da6a416800071498/B1304.pdf

Emmerth, P.P. and Bayne, D.R. (1996). Urban influence on phosphorus and sediment loading of West Point Lake, Georgia. *Water Resources Bulletin*, 32:145-154.

EPA. (1995). Federal Register Vol. 60, No. 189. U.S. Environmental Protection Agency. Washington DC.

EPA. (2006). Framework for Developing Suspended and Bedded Sediments (SABS) Water Quality Criteria. EPA-822-R-06-001. Office of Water. U.S. Environmental Protection Agency. Washington DC.

EPA. (2008). Introduction to the Clean Water Act. U.S. Environmental Protection Agency. Retrieved 12 July 2011 from: http://www.epa.gov/owow/watershed/wacademy/acad2000/cwa/right1.htm.

EPA. (1994). What is nonpoint source (NPS) pollution? EPA-841-F-94-005. U.S. Environmental Protection Agency. Retrieved 10 July 2011 from: http://www.epa.gov/owow/nps/qu.html.

Fenneman, N.M. (1938). Physiography of Eastern United States. McGraw-Hill Book Company, New York.

Giardino, C., Pepe, M., Brivio, P.A., Ghezzi, P. Zilioli, E. (2001). Detecting chlorophyll, secchi disk depth, and surface temperature in a sub-alpine lake using Landsat imagery. *Science for the Total Environment* 286:19-29.

Glysson, G.D., Gray, J.R.., Conge, L.M. (2000). Adjustment of total suspended solids data for use in sediment studies: Proceedings, ASCE's 2000 Joint Conference on Water Resources Engineering and Water Resources Planning and Management, July-31-August 2, 2000. Minneapolis, Minnesota.

Griffith, J.A. (2002). Geographic techniques and recent applications of remote sensing to Landscape-water quality studies. *Water, Air, and Soil Pollution,* 138: 181-197.

Hambrook Berkman, J.A.., Canova, M.G. (2007). Algal biomass indicators: U.S. Geological Survey Techniques of Water-Resources Investigations, book 9, chap. A7, section 7.4, Retrieved 14 March 2011 from: http://pubs.water.usgs.gov/twri9A/

Han, L., Jordan, K. (2005). Measuring algal chlorophyll concentration in Pensacola Bay, Florida using Landsat ETM+ data. *International Journal of Remote Sensing* 26 (23): 5245-5254.

Han, L. (1997). Spectral reflectance with varying suspended sediment concentrations in pure and algal-laden waters. *Photogrammetric Engineering and Remote Sensing* 63 (6): 701-705.

Jenson, J.R. (2000). *Remote Sensing of the Environment: An Earth Resource Perspective*. New Jersey: Prentice Hall.

Kloiber, S. M., Brezonik, P. L., Bauer, M. E. (2002). Application of Landsat imagery to regional-scale assessments of lake clarity. *Water Research* 36: 4330–4340.

Kloiber, S.M., Brezonik, P.L., Olmanson, L.G., Bauer, M.E. (2002). A procedure for regional lake water clarity assessment using Landsat multispectral data. *Remote Sensing of Environment* 82: 38-47.

Lathrop, R.G. (1992). Landsat Thematic Mapper monitoring of turbid inland water quality. *Photogrammatric Engineering and Remote Sensing* 58:465–470.

Liu, Y., Islam, M., Gao, J. (2003). Quantification of shallow water quality parameters by means of remote sensing. *Progress in Physical Geography* 27 (1): 24-43.

Moran, M.S., Jackson, R.D., Slater, P.N., Tellit, P.M. (1992). Evaluation of simplified procedures for retrieval of land surface reflectance factors from satellite sensor output. *Remote Sensing of Environment* 41:169-184.

Nas, B. Ekercin, S., Karabork, H., Berktay, A., Mulla, D.J. (2010). An application of Landsat-5 TM image data for water quality mapping in Lake Beysehir,Turkey. *Water Air Soil Pollution* 212 (1): 183-197.

National Academy of Sciences. (1969). *Eutrophication: Causes, Consequences, Correctives.* Proceedings of a Symposium. National Academy of Sciences. Washington D.C.

NSF. (2004). 2004 Fluorometric determination of chlorophyll-*a*, Arctic Long Term Ecological Research protocol. National Science Foundation, Toolik Field Station. Fairbanks, AK. Retrieved 12 August 2011 from: http://ecosystems.mbl.edu/arc/streams/ protocol2.html.

Novo, E.M.M., Steffen, C.A., Braga, C.Z.F. (1991). Results of a laboratory experiment relating spectral reflectance to total suspended solids. *Remote Sensing of the Environment* 36:67-72.

Omernik, J.A. (1989). Ecoregions of the conterminous United States. *Annals of the Association of American Geographers* 77:118-125.

Raschke, R.L. (1993). Guidelines for Assessing and Predicting Eutrophication Status of small Southeastern Piedmont Impoundments. Environmental Services Division, Ecological Support Branch, U.S. Environmental Protection Agency Region IV. Athens, GA.

Ritchie, J.C., Schiebe, F.R., McHenry, J.R. (1976). Remote sensing of suspended sediments in surface water. *Photogrammetric Engineering and Remote Sensing* 42 (2): 1539-1545.

Ritchie, J.C.,Cooper, C. M., Schiebe, F. R. (1990). The Relationship of MSS and TM digital data with suspended sediments, chlorophyll, and temperature in Moon Lake, Mississippi. *Remote Sensing of the Environment* 33:137-148.

Ritchie, J.C., Cooper, C.M., Yongqing, J. (1987). Using Landsat multispectral scanner data to estimate suspended sediments in Moon Lake, Mississippi. *Remote Sensing of the Environment* 23:65-81.

Ritchie, J.C., Zimba, P., Everitt, J. (2003). Remote sensing techniques to assess water quality. *Photogrammetric Engineering and Remote Sensing* 69 (6): 695-704.

Rose, S. (2002). Comparative major ion geochemistry of Piedmont streams in the Atlanta, Georgia region: Possible effects of urbanization. *Environmental Geology*, 42: 102-113.

Schiebe, F.R., Harrington, J.A. Jr., Ritchie, J.C. (1992). Remote sensing of suspended sediments: The Lake Chicot, Arkansas project, *International Journal of Remote Sensing* 13(8):1487-150

Skirvin, S. (2000). Atmospheric and Radiometric correction of Landsat Thematic Mapper data using the COST Model of Chavez, 1996. Tuscon, Arizona Remote Sensing Center, University of Arizona. Retrieved 10 April 2011 from: http://arcs.arid.arizona.edu/ resources/image-processing/landsat/ls5-atmo.html.

Szabo, M.N., Osborne, E.N., Copeland, C.N. Jr., Neathery, T.L. (1988). Geologic Map of Alabama, Geological Survey of Alabama Special Map 220, Scale 1:250,000.

Thornwaite, C.W. (1948). An approach toward rational classification of climate. *Geographical Review* 38: 55-94.

Tiwary, R.K., B.B. Dhar. (1994). Environmental pollution from coal mining activities in Domadar River Basin, India. *Mine Water and the Environment* 3: 1-10.

USDA. (1982). Soil Survey: Jefferson County, AL. USDA, Soil Conservation Service. Series 1949.

Wahl, M.H., McKellar, H.N.,Williams, T.M. (1997). Patterns of nutrient loading in forested and urbanized coastal streams. *Journal of Experimental Marine Biology and Ecology*, 213:111-131.

Wang, F., Han, L., Kung, T., Van Arsdale, R.B. (2006). Applications of Landat-5 TM imagery in assessing and mapping water quality in Reelfoot Lake, Tennesse. *International Journal of Remote Sensing* 27: 5269-5283.

World Bank Group. (1998). "Pollution Prevention and Abatement Handbook: Coal Mining and Production." Environmental Department, Washington DC.

Zhang, Y., Wang, Y. () Assessment of the Impact of Land-Use Types on the Change of Water Quality in Wenyu River Watershed (Beijing, China). International Perspectives of Environmental Change 14: 275-294.

Zhou, W., Wang, S., Zhou, Y., Troy, A. (2006). Mapping the concentrations of total suspended matter in Lake Taihu, China, using Landsat-5 TM data. *International Journal of Remote Sensing* 27:1177-1

APPENDIX

March 2012 TSS and SDD

A 3rd set of samples were collected in early March 2012 to better understand the threshold of TSS directly post rain event. The week prior to sampling the study area received over 1.2 inches of rain and at the time of sampling the discharge was 4,230 ft^3s^{-1}. Results confirm March 2011 TSS values were relatively low and indicate that directly after a rain event TSS conditions increase significantly. This data was not used in remote sensing correlation/regression modeling.

Table 22 March 2012 TSS and SDD

Sample	TM Band 1	TM Band 2	TM Band 3	TM Band 4
1	0.021	0.021	0.019	0.017
2	0.023	0.024	0.021	0.020
3	0.021	0.024	0.017	0.020
4	0.021	0.021	0.017	0.013
5	0.019	0.018	0.017	0.013
6	0.019	0.021	0.017	0.020
7	0.021	0.021	0.017	0.013
8	0.019	0.021	0.019	0.017
9	0.018	0.018	0.017	0.017
10	0.018	0.018	0.014	0.017
11	0.018	0.018	0.014	0.020
12	0.018	0.021	0.019	0.017